NEG.

N.H.

[redacted]

JET PROPULSION LABORATORY
CALIFORNIA INSTITUTE OF TECHNOLOGY
PASADENA 3, CALIFORNIA

National Aeronautics and Space Administration
Contract No. NASw-6

External Publication No. 647

TEMPERATURE CONTROL IN THE EXPLORER SATELLITES AND PIONEER SPACE PROBES

E. P. Buwalda
A. R. Hibbs
T. O. Thostesen

Copy No. 10

JET PROPULSION LABORATORY
California Institute of Technology
Pasadena 3, California
May 7, 1959

CONTENTS

FIGURES

FIGURES (Cont'd)

FIGURES (Cont'd)

FIGURES (Cont'd)

ABSTRACT *

The Jet Propulsion Laboratory participated in the launching of the EXPLORER satellites and the JUNO II space probes (PIONEERS III and IV). This participation included payload design and the method of achieving temperature control. This Publication describes the basic theory for the passive temperature control of satellites and space probes and the application of this process to the EXPLORERS and PIONEERS III and IV. Some results of in-flight temperature measurements are also presented.

*This paper presents the results of one phase of research carried out at the Jet Propulsion Laboratory, California Institute of Technology, under Contract No. NASw-6, sponsored by the National Aeronautics and Space Administration.

I. INTRODUCTION

The control of the temperature of a satellite or space probe is, in principle, a very simple problem. The temperature is determined only by the amount of radiative heat which the body receives, the heat generated internally, and the heat which the body re-radiates or reflects to the surrounding empty space. The body is not in contact with an atmosphere of any appreciable density.

Thus, in principle, it would be possible to achieve almost any temperature in a satellite or space probe and to hold it at an almost exactly constant value, without recourse to refrigerating or heating devices. Only simple mechanisms would be required in order to adjust a system of reflecting or absorbing screens on the outer surface.

However, in a minimum-weight vehicle, such as the EXPLORERS and PIONEERS, even such simple mechanisms as these are too costly - in terms of weight - to permit their use. It is necessary to use a completely passive technique to achieve the necessary temperature control.

For the EXPLORERS and PIONEERS, the temperature restrictions are imposed by the electronic equipment carried in the instrument section. At temperatures below about -5° C, the batteries cease to operate properly. However, if the temperature were to fall below this limit, no permanent damage would be done. The equipment would function properly if it were warmed up again.

At temperatures above +50° C, the electronic equipment does not operate properly. However, it does not suffer permanent damage until the temperature exceeds +80° C.

Therefore, the aim of the temperature-control technique was to attempt to hold the temperature of the electronic equipment between the limits of -5° C and +50° C; but, in any event, the temperature was never to exceed +80° C.

The only completely passive technique available is that of covering the outer surface with materials which have the proper radiative characteristics. Even when the surface is prepared in the best possible way, some temperature variation is inevitable for a satellite.

As the satellite moves in its orbit, it passes alternately between sunlight and shadow. The period of this cycle is, of course, the period of one revolution around the earth, or about 1 1/2 to 2 hr. This wide variation could be avoided only if a high inclination of the orbit to the equator were attained, thus keeping the satellite continuously in sunlight.

Fortunately, the equipment within the satellite need not experience the same degree of variation as the shell. Tests on a prototype model showed that the electronic equipment could be so well insulated from the shell that its temperature varied only a few degrees; whereas, the fluctuations in shell temperature exceeded 100° C between extremes.

In this case, the temperature of the electronic equipment stays near the average temperature of the shell, averaged over one orbit. However, as the orbit regresses around the earth, as the line of apsides precesses about the orbit, and as the earth turns about the sun, this average temperature varies. Furthermore, the attitude of the satellite with respect to the sun is also important since the

EXPLORER is roughly cylindrical in shape.

Thus, it is necessary to:

1. Find surface materials which will maintain the average temperature of the shell within the prescribed boundaries, keeping in mind the long-term variations caused by the motion of the plane of the orbit, the line of apsides, and the earth.
2. Launch at the right time of day in order to achieve the proper attitude of the satellite with respect to the sun; or select surface properties consistent with a prescribed launching time.
3. Insulate the electronic equipment from the shell (for the satellite).

This Publication outlines the mathematical development of the heat-flux equation for the shell. The result shows how the temperature of the shell depends on surface characteristics, position of the orbital plane, and attitude of the vehicle. This outline is followed by a discussion of the surface-characteristics problem and a description of the materials used on the surfaces of the EXPLORERS and PIONEERS.

A comparison is given of the predicted and observed temperatures of the electronic equipment, and a presentation of all of the temperature data received from EXPLORER I -- 1958 alpha, and PIONEERS III and IV, all of which were designed and fabricated at the Jet Propulsion Laboratory.

II. ANALYSIS OF THE TEMPERATURE OF THE SATELLITE SHELL

A. Mathematical Development

The rate of change of the temperature of the shell of a satellite is

$$\frac{dT_p}{dt} = \frac{I_S + I_E - R}{mc} \tag{1}$$

where

T_p = the temperature of the shell

I_S = the radiative power absorbed from sunlight

I_E = the power received from thermal radiation of the earth

R = the power radiated from the shell

t = time

mc = the total heat capacity of the shell

The use of the total heat capacity of the shell implies that the assumption has been made that all parts of the shell are in good thermal contact with each other; that is, it is assumed that the rate of heat transfer by conduction from one part of the shell to another is much greater than the rate of heat transfer by radiation between the surface of the shell and the surrounding environment.

It also implies a second assumption; namely, that the electronic equipment on the interior is so well insulated from the shell that it can have no effect on the temperature of the shell over the time periods of importance. The first assumption is valid, but the second is somewhat questionable. Actually, the temperature of the internal equipment did vary several degrees in the period of one orbit; hence hence it did have an effect on the shell temperature. However, the

effect on the average shell temperature is not great; consequently, for the present problem, it is probably not worth the added complexity to introduce this effect.

Solar radiation is received by the satellite in two ways. First, radiation is received directly from the sun at the rate

$$I_{S_1} = A_S \alpha_1 S \tag{2}$$

where

A_S = the projected area of the satellite as seen from the direction of the sun

α_1 = the coefficient of absorptivity of the shell for solar radiation

S = the solar constant = 1.94 cal/cm^2/min

The projected area of the satellite for the receipt of direct solar radiation is, naturally, a function of the shape of the satellite. In the present analysis it has been assumed that the portion of the satellite body which is important for temperature control has the following characteristics: (1) It has a conical nose. (2) The base of this cone is attached to a cylindrical section of the same radius. (3) The combined surface of the cone and cylinder is exposed to radiative heat transfer with the surrounding environment. (4) The base of the cylinder is thermally insulated from the remainder of the payload and acts as a radiation shield for this base area. A sketch of this configuration is shown in Fig. 1. The projected area of the satellite for the receipt of radiation is a function of the angle of orientation η shown in Fig. 1.

In order to determine this angle for the receipt of radiation from any particular source (e.g., the sun), it is necessary to make some assumptions about the motion of the satellite.

EXPLORER I was launched into orbit spinning about its longitudinal axis. If it were a rigid body, it would maintain this spin orientation for a considerable period of time, since no appreciable external torques are acting perpendicular to the angular momentum vector.

However, EXPLORER I is not a rigid body. Extending from its sides are four wire antennas (aircraft control cables). The flexing of these wires introduces appreciable internal damping. Since no external torques are applied by this flexing, the angular momentum must stay fixed in both direction and magnitude.

The only way that energy can be dissipated is for the mode of spinning to change, eventually reaching a minimum energy mode for constant angular momentum.

This is what happened. Within a day after launch, EXPLORER I was rotating end over end about a transverse axis, with the angular momentum vector still pointing in the original direction.

Since the angular momentum vector maintains a fixed direction in Newtonian space, it is convenient to define the orientation of the satellite with respect to this direction. Since the spin around this vector takes place within a period much shorter than any thermal time constants important for this problem, the area of the satellite is averaged over the angles η traversed in one spin cycle.

Let η_1 be the angle between the angular momentum vector and the direction of a source of radiation. Let ξ be the angle between the

longitudinal axis of the satellite and the plane defined by the angular momentum vector and a line from the satellite to the radiation source. Then for a motion consisting of spin about a transverse axis, the average area is

$$A(\eta_1) = \frac{1}{\pi} \int_0^{\pi} A(\eta)\, d\xi$$

where η is defined by $\cos \eta = \cos \xi \sin \eta_1$, and the function $A(\eta)$ for the conical section configuration of the EXPLORER is shown in Fig. 2, where its ratio with the total surface area A_T is plotted as a function of η. For the cylindrical section, this function is simply $2rl_3 \sin \eta$.

If the source of radiation is the sun, then $\eta_1 = \eta_S$.

The satellite will also receive solar radiation which is reflected from the earth. The radiative power received by the satellite through reflection from an element dS of the earth's surface area is

$$dI_{S_2} = (P.A.)\, \alpha_1\, i(\alpha) \cos \alpha \cos \beta \frac{dS}{\rho^2} \tag{3}$$

where

P.A. = projected area of the satellite seen from the surface area dS

$i(\alpha)$ = the radiative power reflected at an angle α to the normal of the surface element with primary radiation normal to the element

β = the angle between the direction of the sun and the normal to the surface element dS

ρ = the distance between the surface element and the satellite

The geometry of the earth-to-satellite radiation process is shown in Fig. 3.

Since the satellite shape under consideration has cylindrical symmetry only, each surface element of the earth will see a different projected area of the satellite. Thus, the angle of orientation η_1 will be a variable in the subsequent integration of dI_{S_2}.

Let dS cos α be the surface element of a sphere of radius ρ. Then

$$dS \cos\alpha = \rho^2 \sin\eta_1 \, d\eta_1 \, d\psi$$

where η_1 and ψ are spherical polar coordinates about the center of the satellite with the polar axis coinciding with the direction of the angular momentum vector of the body. Rewriting Eq. (3) in terms of η_1 and ψ gives

$$dI_{S_2} = \frac{A_S}{A_T} \alpha_1 i \cos\gamma \sin\eta_1 \, d\eta_1 \, d\psi$$

where γ is defined as the angle between the direction of the sun and the normal to the surface element $\rho^2 \sin\eta_1 d\eta_1 d\psi$.

With the help of Fig. 4, it can be seen that

$$\cos\gamma = \cos\theta_S \left[\cos(\eta_0-\eta_1) - \sin(\eta_0-\eta_1)\operatorname{ctn}\eta_0\right] + \cos\eta_S \sin(\eta_0-\eta_1)\csc\eta_0$$

where

θ_S = the angle between the radius vector from the center of the earth to the satellite and the direction of the sun

η_S = the angle between the direction of the angular momentum vector of the satellite and the direction of the sun

η_0 = the angle between the direction of the angular momentum vector of the satellite and a radius vector from the center of the earth to the satellite

The assumption has been made that i is independent of α; that is, that the reflection from the earth is perfectly diffuse.

The total power received by the satellite through reflection may now be written as

$$I_{S_2} = 2\alpha_1 \int_0^{\pi} \int_0^{\psi_1} \frac{A_S}{A_T} \sin\eta_1 \{\cos\theta_S [\cos(\eta_0-\eta_1) - \sin(\eta_0-\eta_1)\,\mathrm{ctn}\,\eta_0] + \cos\eta_S \sin(\eta_0-\eta_1)\csc\eta_0\}\, d\eta_1 d\psi \tag{4}$$

where the limits of integration over ψ depend on η_1 and η_0

$$\cos\psi_1 = -\,\mathrm{ctn}\,\eta_0\,\mathrm{ctn}\,\eta_1 \quad \text{for } \eta_1 > \left[\frac{\pi}{2} - \eta_0\right]$$

$$\psi_1 = \pi \quad \text{for } \eta_1 < \left[\frac{\pi}{2} - \eta_0\right]$$

Integration with respect to ψ is immediate; however, the mathematical form of the ratio A_S/A_T as a function of η_1 is too complex to permit analytical integration. Therefore, the integration with respect to η_1 must be carried out numerically.

In the above integration, it has been assumed that the earth is flat; hence, the earth as seen from the satellite covers half of the sky. In an earlier study by Dr. A. R. Hibbs of the Jet Propulsion Laboratory (Ref. 1) the total power received by a spherical satellite through reflection was found to be

$$I_{S_2} = 2\pi^2 a^2 \alpha_1 i (1-\sqrt{2y}) \cos\theta_S$$

through the first order in y, where

$y = h/r_0$

h = height of the satellite above the earth's surface

r_0 = radius of the earth

The factor $(1 - \sqrt{2y})$ cuts down the fraction of the sky filled by the earth, and can be thought of as the altitude effect.

Assuming that the altitude effect is independent of the shape of the satellite, the results of the integration of Eq. (4) are corrected by the factor $(1 - \sqrt{2y})$.

If the integral over the term with the coefficient $\cos\theta_S$ is called $A_{r_1}(1 - \sqrt{2y})^{-1}$, and of the integral over the term with the coefficient $\cos\eta_S$ is called $A_{r2}(1 - \sqrt{2y})^{-1}$, then the result for the power received from sunlight is

$$I_{S_2} = \alpha_1 i \pi [A_{r_1} \cos\theta_S + A_{r_2} \cos\eta_S] \quad (5)$$

Referring to Figs. 3 and 4, it can be seen that

$$\cos\theta_S = \cos\theta \cos\phi$$

$$\cos\eta_S = \cos\phi \cos(\eta_0 - \theta)$$

where

θ = polar angle of the satellite in its orbit measured from noon transit

φ = the angle between a radius vector from the center of the earth to the sun and the plane of the satellite orbit

Substituting these relationships in Eq. (5) gives

$$I_{S_2} = \alpha_1 i \pi \cos\phi \, [A_{r_3} \cos\theta + A_{r_4} \sin\theta] \tag{6}$$

where

$$A_{r_3} = A_{r_1} + A_{r_2} \cos\eta_0$$

$$A_{r_4} = A_{r_2} \sin\eta_0$$

The function $i(\alpha)$, appearing in Eq. (3), is defined for the sun vertically above a particular surface element. With this definition the total power radiated from a particular surface element into a hemisphere can be obtained with a simple integration. The result is

$$\pi i = E$$

If the coefficient for diffuse reflection from the earth is r_E, the equation becomes

$$\pi i = S r_E$$

Actually, r_E is not a constant for all surface elements on the earth. For this study an average value over the earth's surface, which is approximately 0.4 (Cf. Ref. 2), is used.

The total power contribution from solar radiation may now be written as

$$I_S = \alpha_1 S [A_S + r_E \cos \Phi (A_{r_3} \cos \theta + A_{r_4} \sin \theta)] \tag{7}$$

Thermal radiation from the earth is received by the satellite at the rate I_E. This term may be evaluated in the same manner as that employed in determining the power contributed from reflected solar radiation. It is not necessary to consider the position of the sun: therefore, the angles θ_S and η_S do not appear in the result of the integration. Use of the Stefan-Boltzmann law yields the following result:

$$I_E = A_E \alpha_2 \sigma T_E^4 \tag{8}$$

where

A_E = the total projected area of the body for receipt of thermal radiation from the earth (based on an integral similar to that of Eq. 4)

σ = the Stefan-Boltzmann constant

T_E = the effective temperature of the earth = 250°K (Ref. 3)

α_2 = the coefficient of absorptivity of the body for receipt of thermal radiation at 250°K

The thermal radiation from the satellite may be written as

$$R = A_T \epsilon_2 \sigma T_P^4 \tag{9}$$

where

A_T = the total surface area of the body

ϵ_2 = the coefficient of emission for thermal radiation from the satellite

For a particular wave length of radiation Kerchoff's law states

$$\epsilon = \alpha$$

We expect the satellite to be at approximately the same temperature as the earth. Therefore, the important wave length region of its radiation should be approximately the same as that of the thermal radiation from the earth, so that to a good approximation

$$\epsilon_2 = \alpha_2$$

The equation for the rate of change of the temperature of the satellite shell may now be rewritten in the following manner

$$\frac{dT_P}{dt} = \frac{A_T}{mc}\left\{\alpha_1 S\left[\frac{A_S^{(1)}}{A_T} + r_E \cos\phi\left(\frac{A_{r_3}}{A_T}\cos\theta + \frac{A_{r_4}}{A_T}\sin\theta\right)^{(2)}\right] + \sigma\alpha_2\left(\frac{A_E}{A_T}T_E^4 - T_P^4\right)\right\} \qquad (10)$$

and the meaning of the superscripts is as follows:

Term (1) is the direct solar radiation term and is to be included only when the satellite is in the sun. That is, the term is to be included only when θ lies between the angles $(2n - 1/2)\,\pi - \theta_2$ and $(2n + 1/2)\,\pi + \theta_2$ where

$$\theta_2 = \sin^{-1}\left[(\sin\theta_1/\cos\varphi)\right] \text{ for } \varphi \le (\pi/2 - \theta_1)$$
$$\theta_2 = \pi/2 \text{ for } \varphi \ge (\pi/2 - \theta_1)$$
$$\theta_1 = \cos^{-1}\left[r_0/(r_0 + h)\right]$$

It has already been noted that the calculation of the reflected sunlight contribution was made for a flat earth as seen from the satellite to less than half of the sky. However, one additional

effect of the earth's curvature still remains. It has been assumed that all of the earth seen by the satellite is illuminated. Actually, as the satellite approaches the twilight zone, this is not the case. Fortunately, the resulting error is small, and can be easily taken care of, at least to a very good approximation.

The reflected sunlight term, with the superscript (2), is to be included only where θ lies between the angles $(2n - 1/2)\pi$ and $(2n + 1/2)\pi$. Thus, the reflected sunlight term is cut off as the satellite passes over the terminator. Inclusion of the complete term on the sunlit side of the terminator implies too much reflected light. Dropping the term completely on the other side implies too little reflected light. The two errors nearly cancel out.

B. Effect of Surface Characteristics

If the satellite were always in the shadow of the earth, its temperature would approach the equilibrium value $T_p = T_E(A_E/A_T)^{1/4}$, independent of the surface characteristics. But, since the satellite spends over half of its life in the sun, this lower limit is never reached. The action of the sunlight raises the temperature.

The effectiveness of sunlight in raising the average temperature can be evaluated in the following way. Suppose the factor α_2 is divided out of the right-hand side of Eq. (10). The two large factors on this side are competing forcing functions. The first, now with the coefficient (α_1/α_2) S, is positive, but acts only part of the time. The second, now with only σ as a coefficient, is negative and is always present.

The result is a cyclic fluctuation of temperature, whose details can be controlled only by controlling the ratio α_1/α_2, once the shape of the satellite has been determined. The correct choice of this ratio for the satellite surface is critical for temperature control.

Actually, since the satellite is spinning with a period much shorter than any of the important thermal time constants, only the average value of α_1/α_2 over the surface is important. For this reason, it is not necessary to find a single material with the correct ratio α_1/α_2 for the whole surface. If two materials can be found whose ratios of α_1/α_2 bracket the desired value, then the surface may be coated with a pattern of these two materials. Selection of the proper fraction of the surface to be covered by each will then permit the correct average ratio to be achieved.

Two surface materials have been considered; steel (since the satellite shell is made of steel) and Rokide[2], a ceramic material, (since the satellite is exposed to aerodynamic heating during the launch phase). A steel surface accepts a relatively large amount of power from solar radiation (high value of α_1/α_2), whereas a Rokide-coated surface accepts a relatively small amount of such power (low value of α_1/α_2). The value of α_1/α_2 for the surface materials to be used must be carefully measured if accurate temperature predictions are required. Such measurements have been made for steel and Rokide surfaces for the Jet Propulsion Laboratory by the Mechanical Engineering Department of the University of California at Berkeley. A discussion of these measurements may be found in Ref. 4.

[2]Rokide A, aluminum oxide applied by a patented process of the Norton Co., Worcester, Mass.

Briefly, the ratio of α_1/α_2 for Rokide was found to be 0.437. Two types of steel were used with two different surface preparations. For the steel used on the cylinder α_1/α_2 is 1.92; whereas, for the steel used in the nose cone the ratio is 4.12.

III. AVERAGE TEMPERATURES OF THE SATELLITE SHELL

The average temperature of the satellite shell may be determined by numerical integration of Eq. (10). It is necessary to specify the time of launch, the angle between the plane of the orbit and the direction of the sun, the characteristics of the orbit, the surface characteristics of the satellite, and the total heat capacity of the satellite payload. A number of such integrations have been carried out to illustrate the effect of the various parameters upon the temperature of the satellite shell. Examples of the average temperatures obtained from these integrations are displayed in Figs. 5 through 8, where

h = the altitude of the circular orbit in miles

φ = the angle between the plane of the orbit and the direction of the sun

δ = the angle around the circular orbit measured from the launching point

EXPLORER I is approximately 80 in. long and 6 in. in diameter (see Fig. 9) and is composed of three sections: the nose cone, the cylindrical section to which the nose cone is attached, and the empty fourth-stage motor case. Each of the three sections is thermally insulated from the others so that the temperature of each section may

be considered independently. Control of the temperature is necessary for only the first two sections since they contain the electronic equipment.

For this study, it was assumed that the thickness of the satellite nose cone shell was 3 mm at the tip and 0.8 mm over the rest of the body. The total heat capacity of the nose cone shell was determined from the weight of this section of the shell (352.2 g) and the specific heat capacity of steel (0.127 cal/g/°C)(Cf. Ref. 5) to be 44.73 cal/°C. The total surface area A_T for the configuration shown in Fig. 1 was found to be 136.097 $in.^2$ Both of these values were used in the numerical integrations performed.

A second set of average temperatures was obtained for the cylindrical section of the shell, with the dimensions shown in Fig. 9. Both ends of the cylinder were assumed to be insulated from the remainder of the payload and to act as radiation shields. Sample average temperature curves for this configuration are shown in Figs. 7 and 8. This cylindrical configuration has a total surface area of 376.991 $in.^2$ and a total heat capacity of 140.6 cal/°C.

On the basis of these calculations, a ratio of 25% Rokide was selected for the cylindrical section, giving an average α_1/α_2 of 1.37; and a ratio of 30% Rokide was chosen for the nose cone, giving an average α_1/α_2 of 1.61.

IV. TEMPERATURE PREDICTIONS

It is essential to provide the proper temperature environment for the radio equipment carried by the satellite for at least the lifetime

of the batteries powering this radio equipment. It is possible to choose the initial temperature of the satellite shell, averaged over the first few orbits, within the proper bounds. This temperature will vary with time due to the precession of the satellite orbit caused by the oblateness of the earth and also due to the change in orientation of the satellite with respect to the sun. The precession of the orbit may be regarded as a change in the angle between the direction of the sun and the plane of the orbit (φ). Changes in the satellite's orientation with respect to the sun may be accounted for by varying the orientation angle η_S. Since the temperature of interest is that inside the satellite, only the mean value of the shell temperature over a cycle is considered.

1958 ALPHA was injected into orbit at 3 hr 55 min 5 sec Greenwich Mean Time on February 1, 1958. The average altitude of the orbit is approximately 900 statute miles, and the angle of inclination of the orbit to the earth's equator is 33.34 deg. This set of launching conditions gives initial values of η_S = 107 deg, and φ = 0 deg.

As pointed out in Sec. II, the original attitude of the axis of symmetry was not maintained. Within a short period of time the satellite had precessed through 90 deg and was tumbling about its original spin axis with a period of approximately 7 sec. Thus, the expected temperature-time history for 1958 ALPHA must utilize a projected area averaged over the tumbling period. The assumption will be made that the precession of the satellite's axis of symmetry occurred in approximately one day. Thus, on February 2 the satellite is tumbling in a plane approximately 16 deg away from the direction of the sun and the effective projected area for the receipt of solar

radiation corresponds to an average angle of orientation of 116 deg. Predicted internal temperatures for this geometrical situation have been prepared for the nose cone and the cylinder. These predicted internal temperatures are plotted with the observed temperature data in a later Section of this Publication.

V. TEMPERATURE FOR 1958 ALPHA

Four direct temperature measurements are made using resistance thermometers. These resistance thermometers are placed as follows:

1. The stagnation-point temperature measured at the top of the nose cone and capable of covering a range of -50°C to +450°C. The approximate accuracy of this measurement is ±20°C.
2. The nose-cone skin temperature measured just forward of the antenna gap and capable of covering a range of -50°C to +220°C. At 50°C the accuracy of this measurement is ±16°C. At 0°C the accuracy is ±18°C.
3. The cylinder skin temperature measured aft on the cylinder and capable of covering a range of -50°C to +110°C. Over the range of -10°C to +80°C the accuracy of this temperature data is ±4°C.
4. The internal temperature of the cylinder measured in the high-powered transmitter and capable of covering a range of -60°C to +110°C. The accuracy of this measurement ranges from ±2°C at T = 0 to 30°C to ±20°C at T = 90°C.

In addition to these direct temperature measurements, indirect measures of internal temperature are available. The internal temperature of the nose cone may be inferred by observing the frequency level of the cosmic-ray measurement channel. Calibrations of the subcarrier oscillator indicate that the internal temperature of the nose cone is known to ±12°C for T = 0 to 25°C and to ±6°C for T = 25 to 50°C.

There is continuous transmission of all telemetry data. The stagnation point temperature and the nose-cone skin temperature measurements are transmitted by the low-powered transmitter. The internal and skin temperatures of the cylinder are transmitted by the high-powered transmitter. The data are recorded at the following locations:

Patrick Air Force Base	28°N Latitude
Earthquake Valley	33°N Latitude
San Gabriel	34°N Latitude
Nigeria	10°N Latitude
Singapore	2°N Latitude

Patrick Air Force Base, Earthquake Valley, and San Gabriel receive approximately four passes a day; Nigeria and Singapore receive about seven passes a day. Data from the low-powered transmitter are received at all stations. Information from the high-powered transmitter is received at Patrick Air Force Base and San Gabriel only.

The telemetry data from some seven hundred and thirty-two passes have been reduced and plotted against time. The time period covered is from February 1, 1958, to April 14, 1958. Individual figures have been prepared for each of the temperature measurements. The predicted

internal temperature for the nose cone and for the cylinder has been added to the plots of these quantities. These data are shown in Figs. 10 through 29.

Both the measured internal temperature in the cylinder and the indirect measure of internal temperature in the nose cone show a range of 35°C. This range is traversed semiperiodically with an apparent period of approximately 2 1/2 days. However, it is very probable that this temperature range is experienced during each orbit. It should be remembered that the maximum fraction of an orbit over which data is recorded is approximately 25%. The records show an internal fluctuation from 0°C to 35°C inside the cylinder and from 5°C to 40°C inside the nose cone.

In completing the temperature predictions some allowance was made for the remaining uncertainties, such as unpredicted variations in attitude and altitude. In making this allowance, a conservative approach was used consistently based on the requirement that in no case was the temperature to exceed +80°C, the value at which the electronic equipment suffers permanent damage. It was estimated that this allowance might contribute as much as 15°C to the simpler prediction. It is this conservative prediction which is shown in the Figures of this report.

Thus, before the firing, it was estimated that the actual temperatures might run as much as 15° below the conservative predictions. The data show that the temperatures were generally about 10° below this conservative prediction.

Shell temperatures ranging from -25°C to 75°C have been observed. An inspection of Figs. 5 through 8 indicates that a temperature variation of 80 to 90°C during one orbit would be expected.

VI. THE PIONEER PROBES

The temperature-control problem for the moon probes, PIONEERS III and IV, differed in several ways from the problem for the EXPLORER satellites. First, it is not possible to regulate the time of firing in accordance with the requirements of temperature control. Time of firing is dictated by trajectory requirements. Second, the earth does not enter, in a significant way, into the temperature problem during the important portions of the flight. Thus, radiation from the earth can be neglected, and a steady-state temperature can be assumed for the calculations, if the attitude can be held fixed. Third, the amount of heat generated internally by the transmitter and other electronic equipment of the PIONEERS is not a negligible source as it was for the EXPLORERS. Fourth, during the flight through the atmosphere of the launching vehicle, the payload is protected by a shroud, thus making possible the use of surface material without the restriction of ability to withstand aerodynamic heating. Fifth, the temperature extremes permitted for this payload were somewhat narrower than those permitted for the EXPLORER payload.

Figure 27 shows a profile of the payload used in PIONEERS III and IV. The Figure shows four reference areas: The nose cone; the cylindrical wrapping around the battery pack (I); the annular base of

the battery pack (II); and the remaining portion of the payload's base (III). To achieve temperature control, each one of these areas was given a different surface treatment.

The successful operation of the payload requires that the temperature lie between the limits of 20°C and 50°C. It was decided to make each of the above-listed areas separately maintain a temperature as close as possible to the midpoint of the limits, 35°C. It was for this reason that each of the areas received a different surface treatment.

The dependence of temperature upon attitude angle η could not be overcome by controlling the time of launch, as was done for the EXPLORER satellites, since the trajectory requirements for a moon probe specify the time of launch to within the nearest few minutes. Several times of launch on a series of days were selected for the vehicle. In this way, allowance was made for the possibility of last-minute delays in the firing schedule. In turn, this required that the surface coating be changed day by day if such postponements became necessary since each new days firing resulted in a different angle, η.

The nose cone was made of fiberglass, and its outer surface was covered with a gold wash. For PIONEER III, 44% of this surface was then striped with white paint. Area 1 was constructed of a gold-plated aluminum-foil shield, with 40% of the area painted black. Area 3 was gold plated and unpainted. Area 4 was sprayed with aluminum paint. Internal construction was so designed that the 3 watts of internally generated heat was conducted principally to Area 4 for radiation out into space.

The observed payload temperature during the flight of PIONEER III is shown in Fig. 28. The temperature rose steadily during the first several hours of flight as the payload moved out from the shadow of the earth and reached a steady state value of approximately 37°C. Based on trajectory and signal-strength information, it is estimated that the angle η giving the attitude between the payload axis and the sun was approximately 91 deg. This angle was considerably greater than had been expected. As a result, the nose cone was somewhat cooler than expected and the remaining area somewhat warmer than expected.

As a result of the surface temperature differences between various sections of the payload, a heat flux occurred between the payload instrument section and the nose-cone shell. Using a reasonable assumption for the radiative transfer between the forward section of the instrument portion and the interior of the nose shell, the observed temperature appears to be almost exactly that expected on the basis of the surface characteristics.

The expected attitude angles for the trajectories of PIONEER IV were different from those of PIONEER III. As a result, for the actual flight day, the gold-covered nose shell was painted 44% black, the gold-plated-aluminum shield of Area 1 was painted 43% white, and Areas 2 and 3 were the same as in the case of PIONEER III.

The expected inclination angle was 103.5 deg and trajectory and signal-strength measurements indicated that this angle was obtained in flight. The measured temperature for PIONEER IV is shown in Fig. 29.

The measurements indicate an equilibrium temperature of 42°C. Calculation of the expected equilibrium temperature for the attitude angle of 103.50 result in an expected temperature of approximately 35°C, which is 7°C lower than measured.

This 7°C discrepancy between calculated and observed temperatures is within the uncertainties expected. These uncertainties arise from many causes, but the principal factor is a lack of complete information on the radiative properties of surface materials and paints used for temperature control.

VII. CONCLUSIONS

From the results obtained in the flights of the EXPLORER satellites and the PIONEER III and IV moon probes, it appears that passive techniques for temperature control are possible at least for trajectories which do not carry the body so far away from the earth's orbit that the solar constant itself is changed appreciably. In order to achieve adequate control by passive techniques, it is necessary to have excellent information on the radiative properties of the materials used for surface preparation. It is also necessary to prevent any change in the nature of the surface between the time it is prepared and the time that the space probe leaves the atmosphere. Even then, after the best information has been obtained on surface properties, and after the greatest care has been taken to ensure that these surface properties will be preserved throughout the launching phase of the flight, discrepancies are still found between calculated and observed temperatures.

When the temperature control limits are established by electronic equipment, the magnitude of the discrepancies so far observed is sufficiently small that no great danger exists of causing the failure of a payload by unforseen temperature variations. However, when biological samples are introduced into the payload, or when the flight trajectory takes the payload either much closer to or much further from the sun, or when the attitude of the payload can neither be controlled nor compensated for, passive temperature control techniques will be of much less value. Certainly, as the program for the exploration of space develops and the payloads to carry out this exploration become increasingly complex, it is essential to look forward to the necessity of introducing active temperature-control schemes.

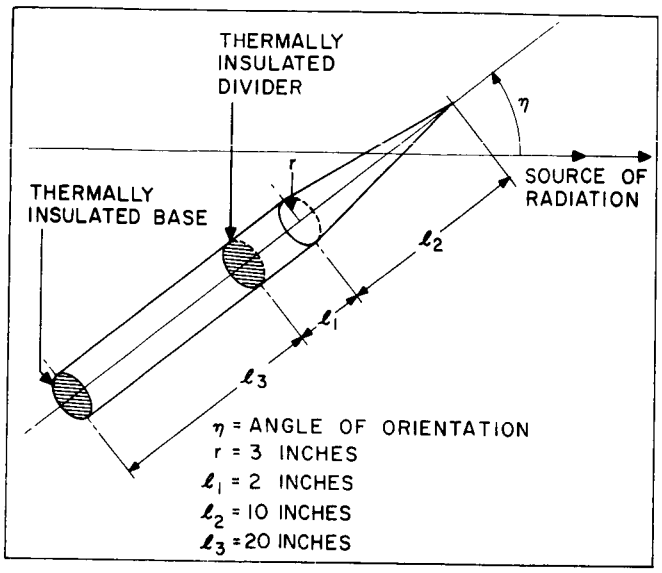

Fig. 1. Dimensions and Orientation of Payload

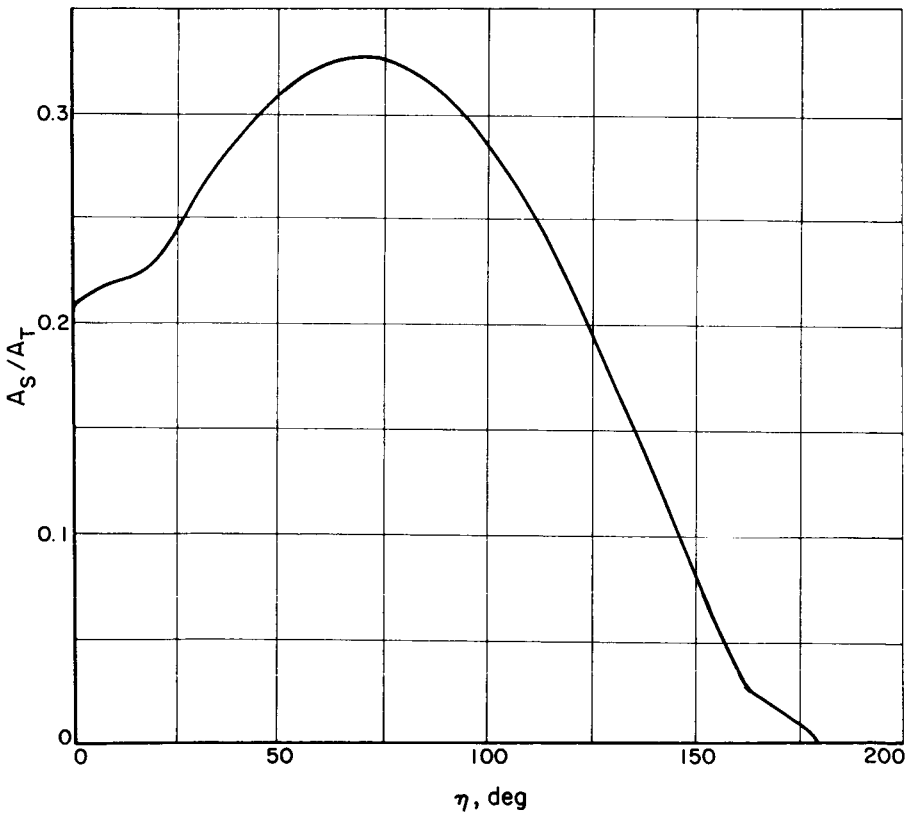

Fig. 2. The Ratio of A_S/A_T for the Conical Section of the Payload

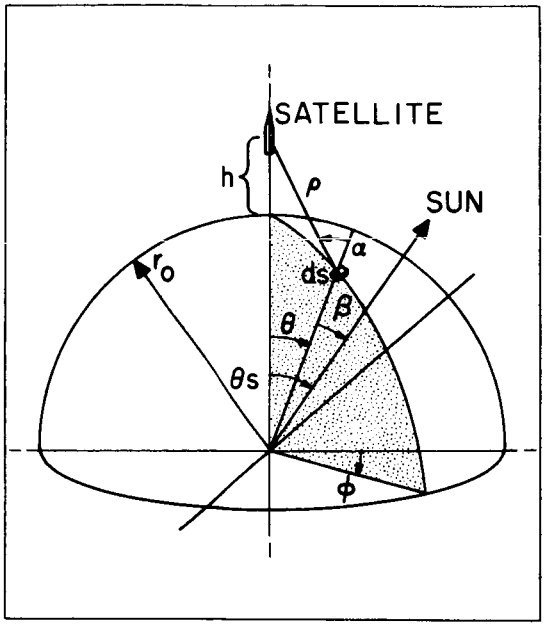

Fig. 3. Geometry of Earth-to-Satellite Radiation Process

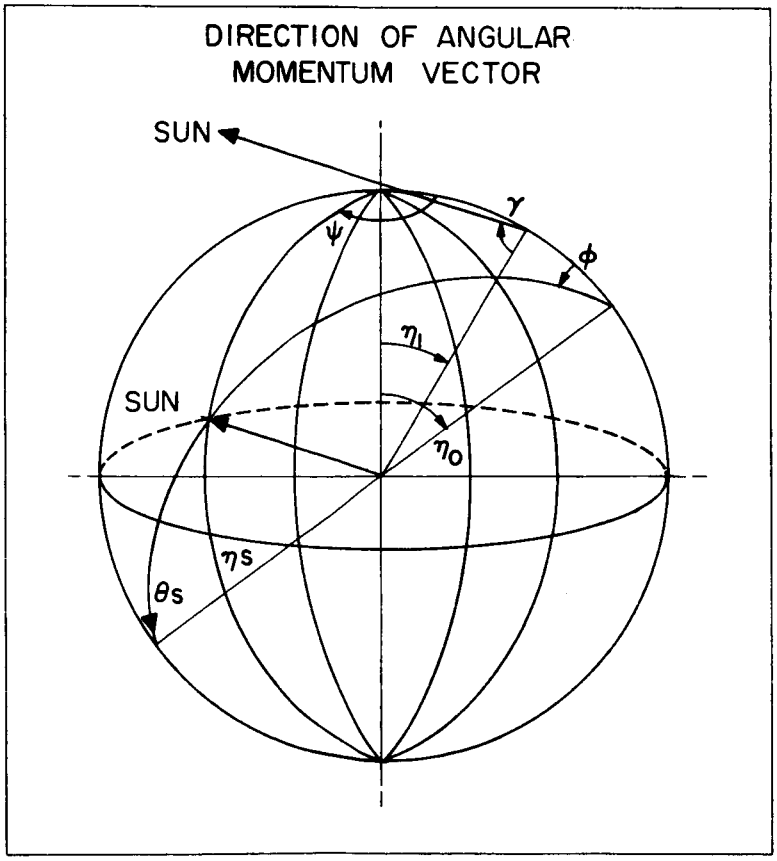

Fig. 4. Relationship Between η_l, ψ Coordinate System and Direction of the Sun

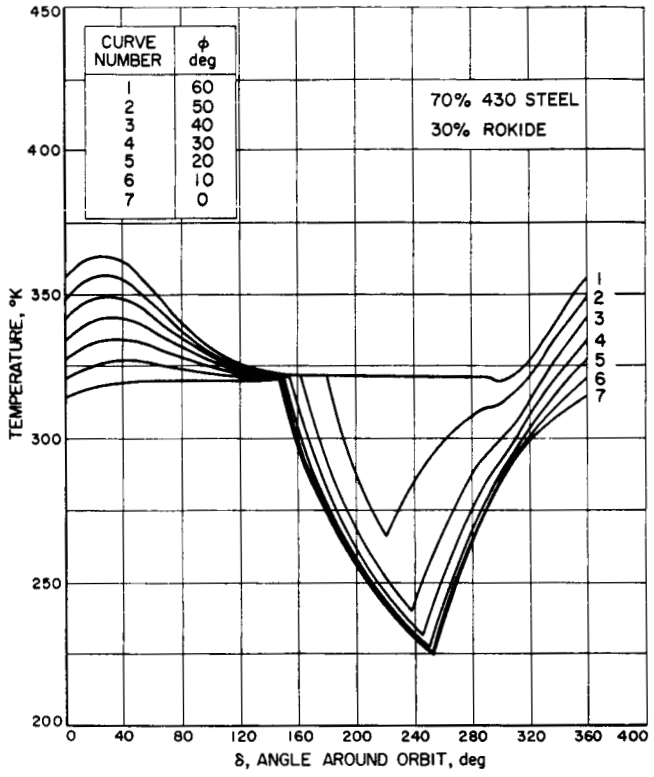

Fig. 5. Average Temperature of Conical Section of the Payload Shell vs Angle Around Orbit for Launch 20° Before Noon Transit, h = 1000 miles, φ = 0°, 10°, 20°, 30°, 40°, 50°, 60°

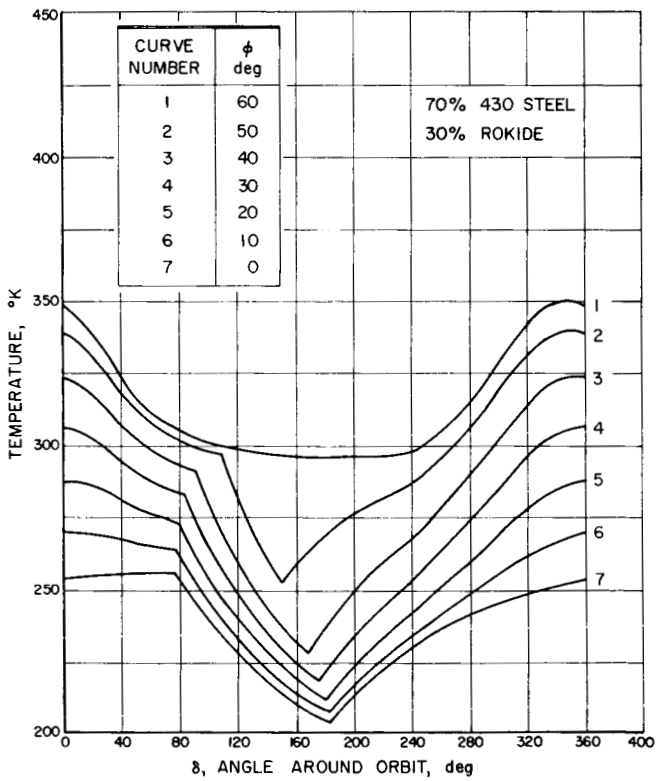

Fig. 6. Average Temperature of Conical Section of the Payload Shell vs Angle Around Orbit for Launch 50° After Noon Transit, h = 1000 miles, φ = 0°, 10°, 20°, 30°, 40°, 50°, 60°

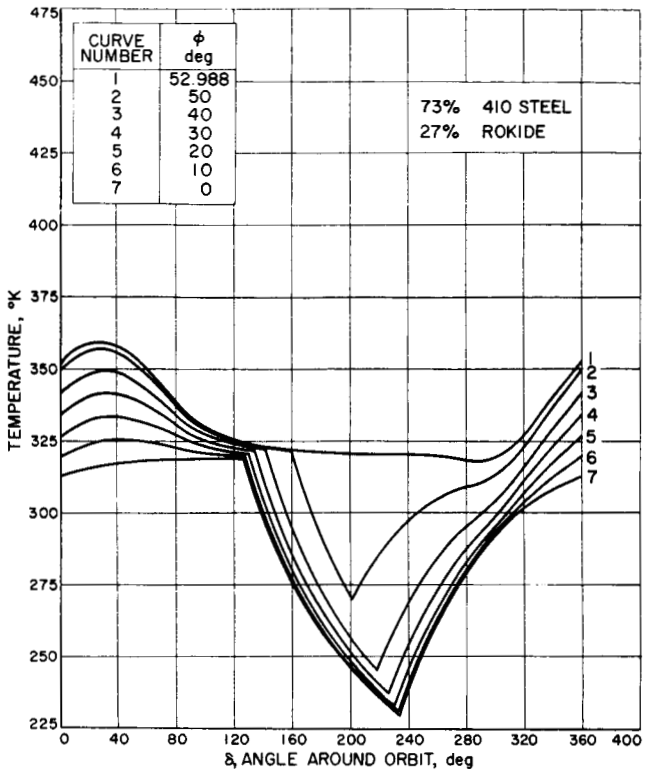

Fig. 7. Average Temperature of Cylindrical Payload Shell vs Angle Around Orbit for Launch at Noon Transit, h = 1000 miles, φ = 0°, 10°, 20°, 30°, 40°, 50°, 60°

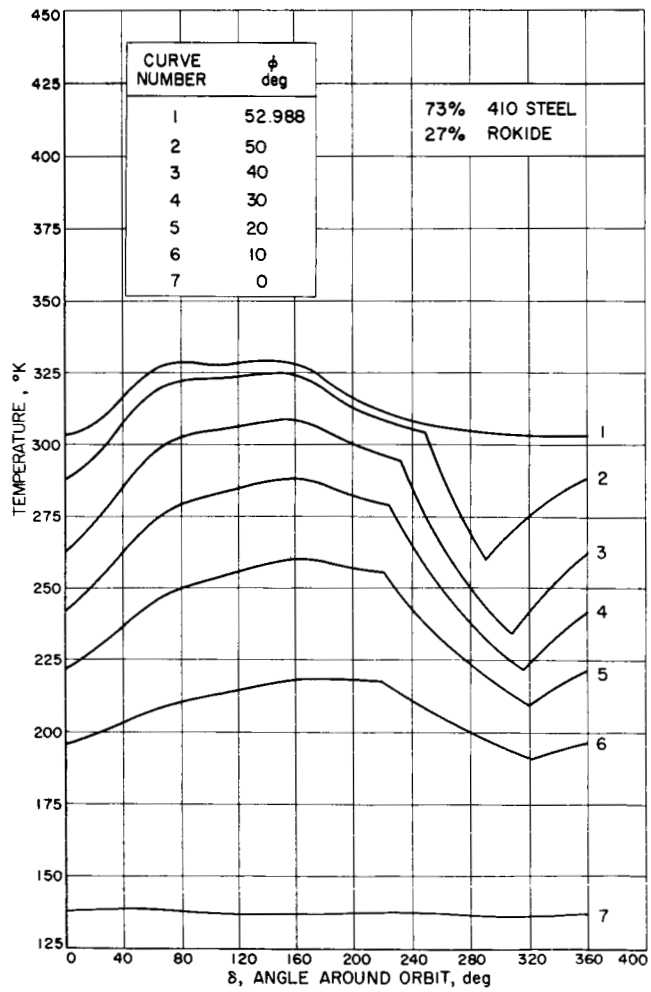

Fig. 8. Average Temperature of Cylindrical Payload Shell vs Angle Around Orbit for Launch 90° Before Noon Transit, h = 1000 miles, φ = 0°, 10°, 20°, 30°, 40°, 50°, 53°

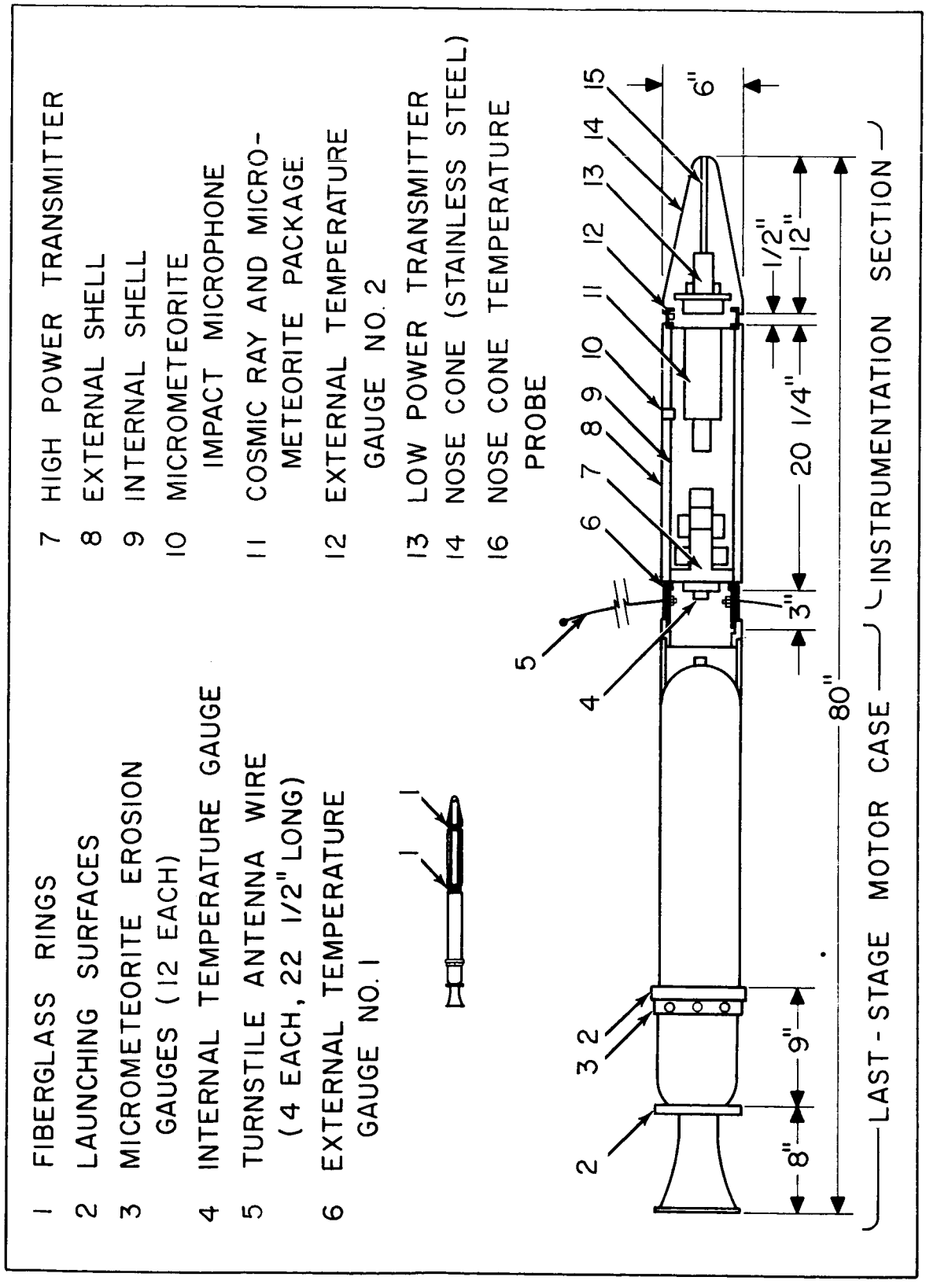

Fig. 9. The Satellite 1958 ALPHA

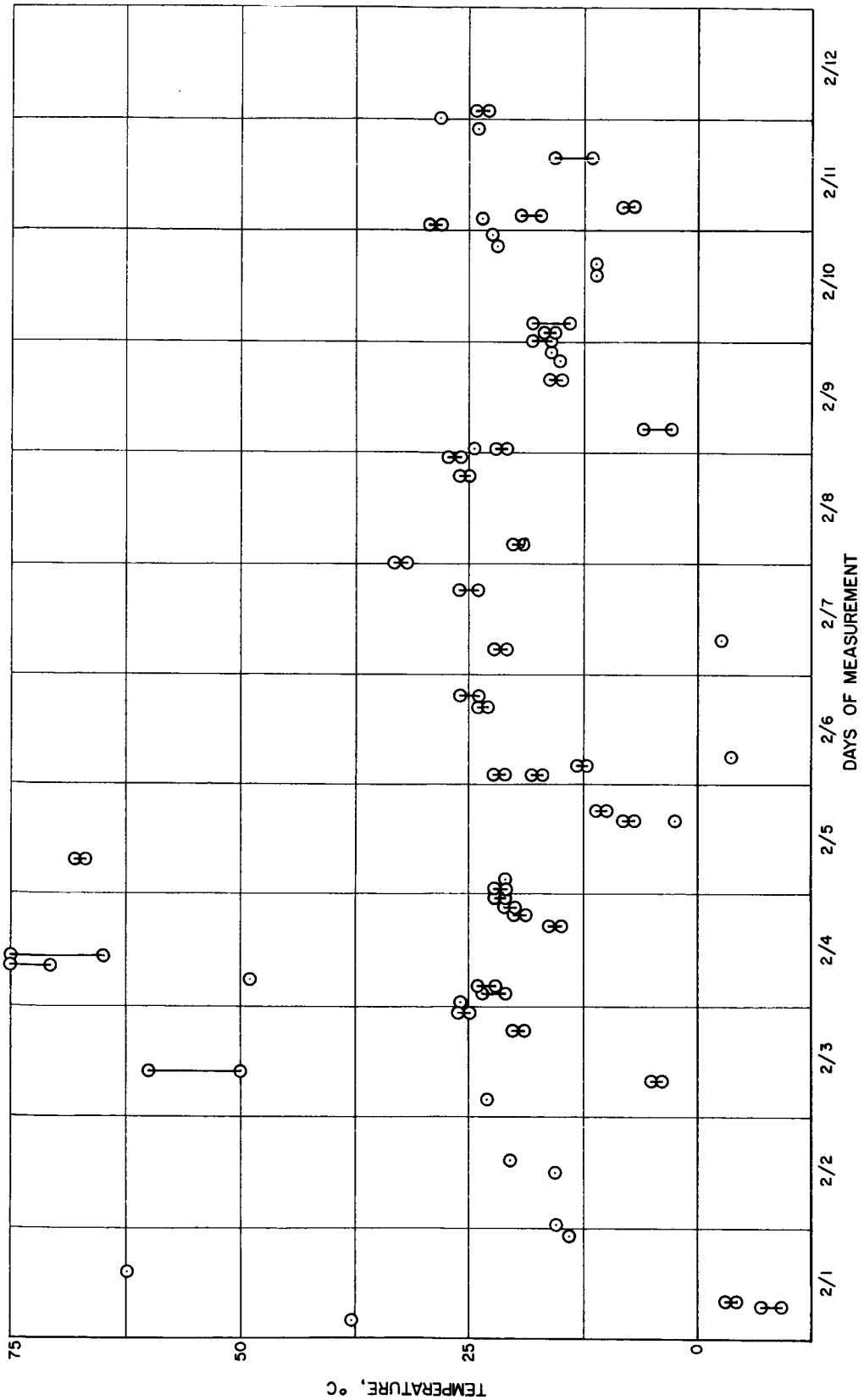

Fig. 10. Measured Cylinder Shell Temperature vs Time for 1958 ALPHA, February 1 through 12, 1958

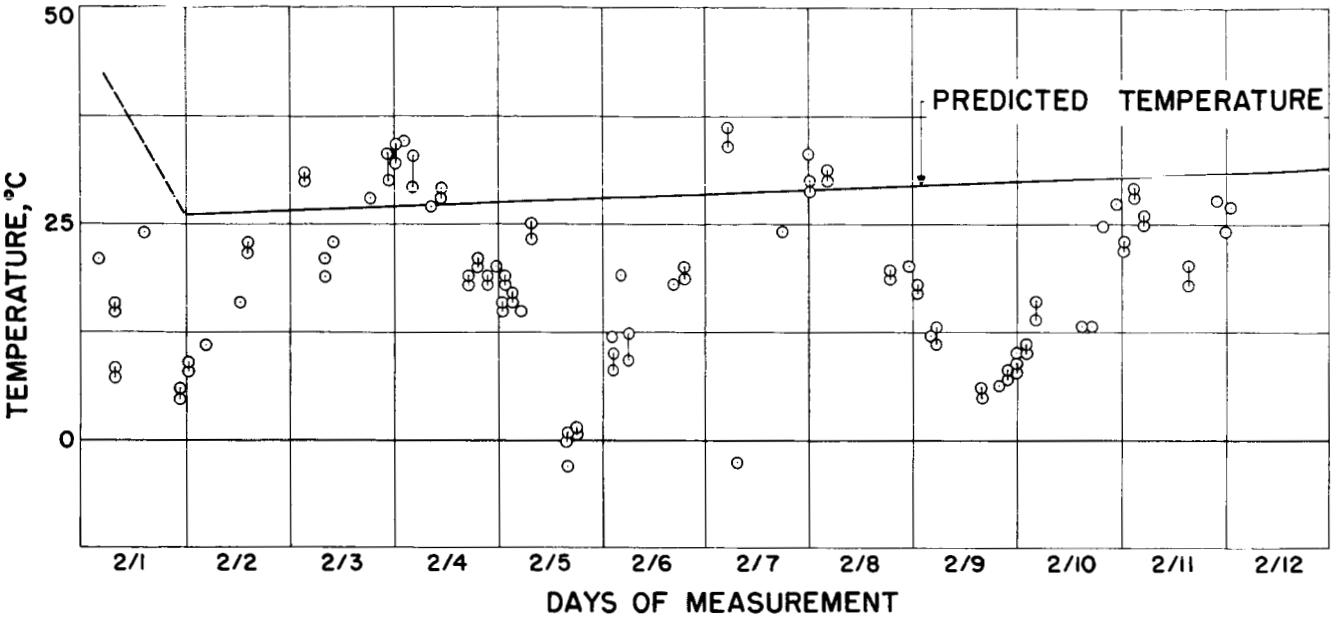

Fig. 11. Measured and Predicted Internal Cylinder Temperature vs Time for 1958 ALPHA, February 1 through 12, 1958

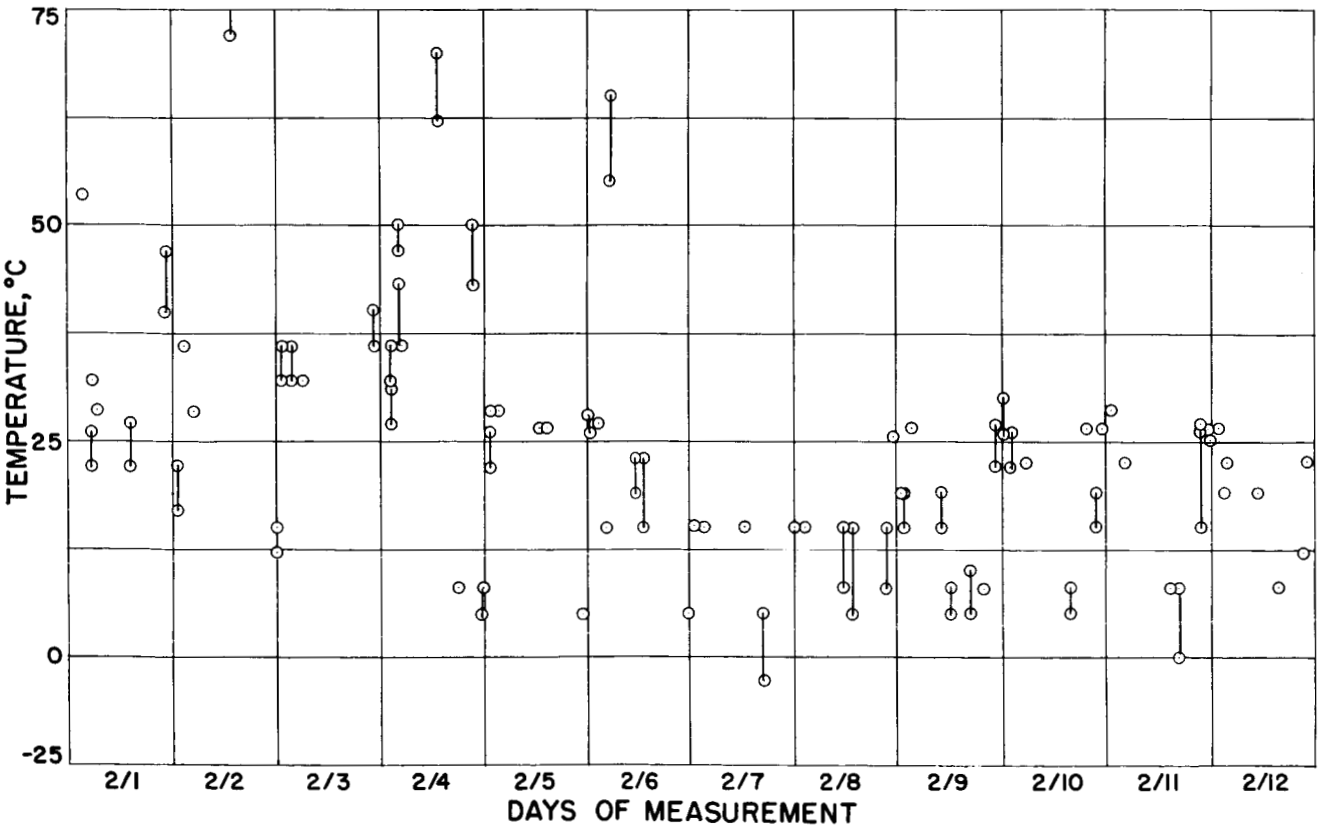

Fig. 12. Measured Cone Shell Temperature vs Time for 1958 ALPHA, February 1 through 12, 1958

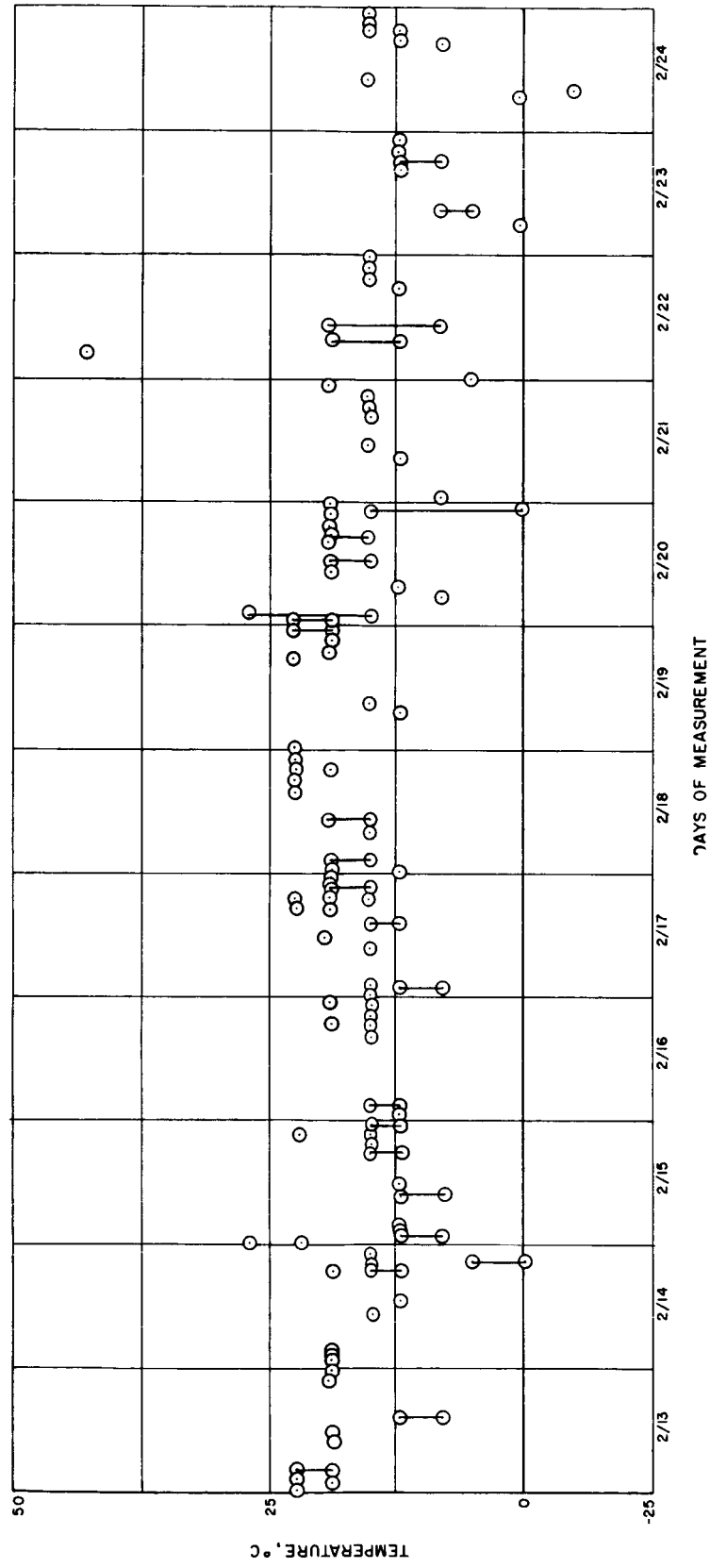

Fig. 13. Measured Cone Shell Temperature vs Time for 1958 ALPHA, February 13 through 24, 1958

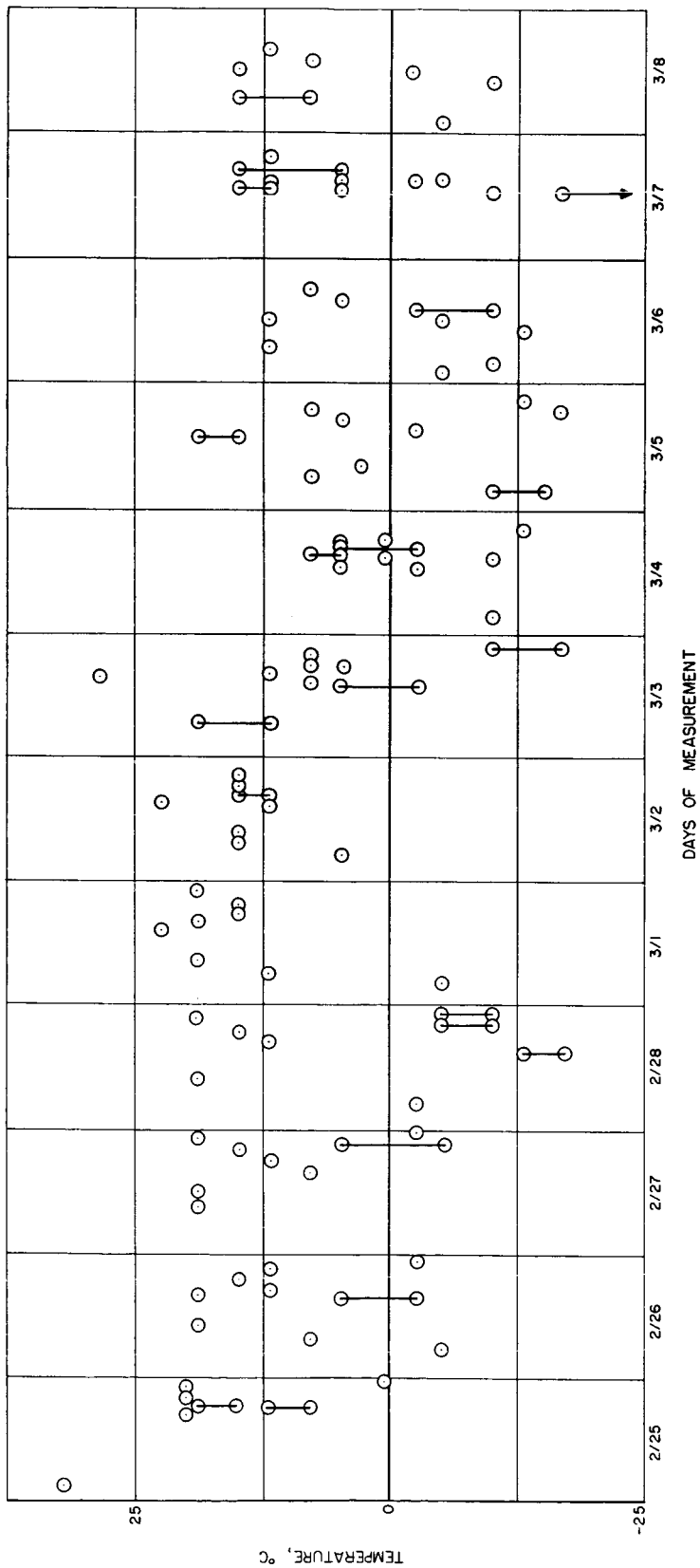

Fig. 14. Measured Cone Shell Temperature vs Time for 1958 ALPHA, February 25 through March 8, 1958

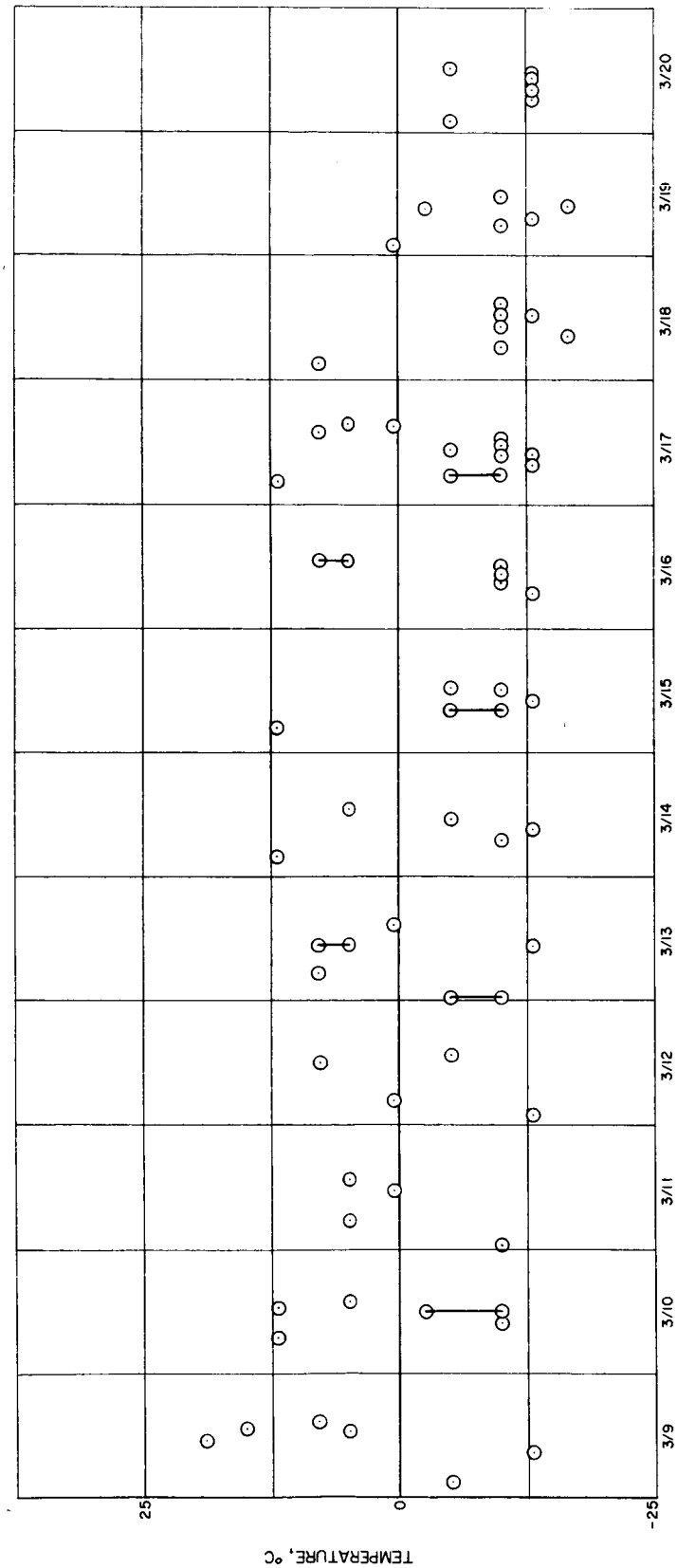

Fig. 15. Measured Cone Shell Temperature vs Time for 1958 ALPHA, March 9 through 20, 1958

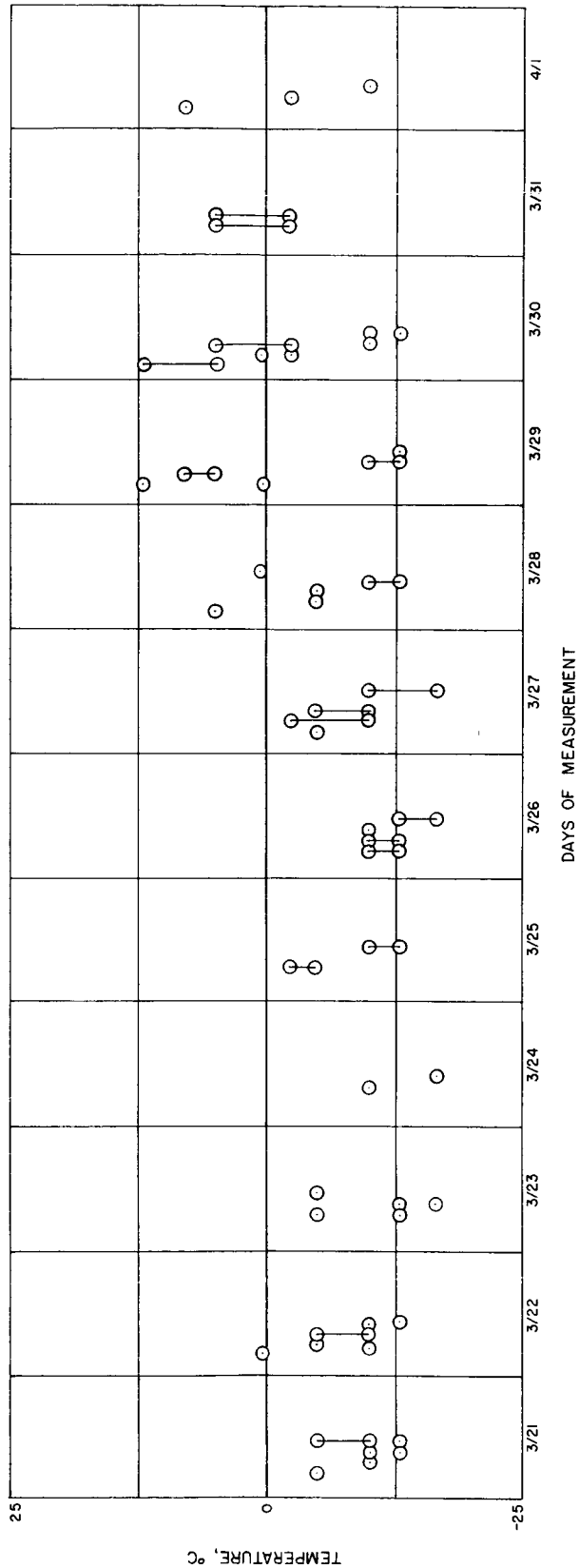

Fig. 16. Measured Cone Shell Temperature vs Time for 1958 ALPHA, March 21 through April 1, 1958

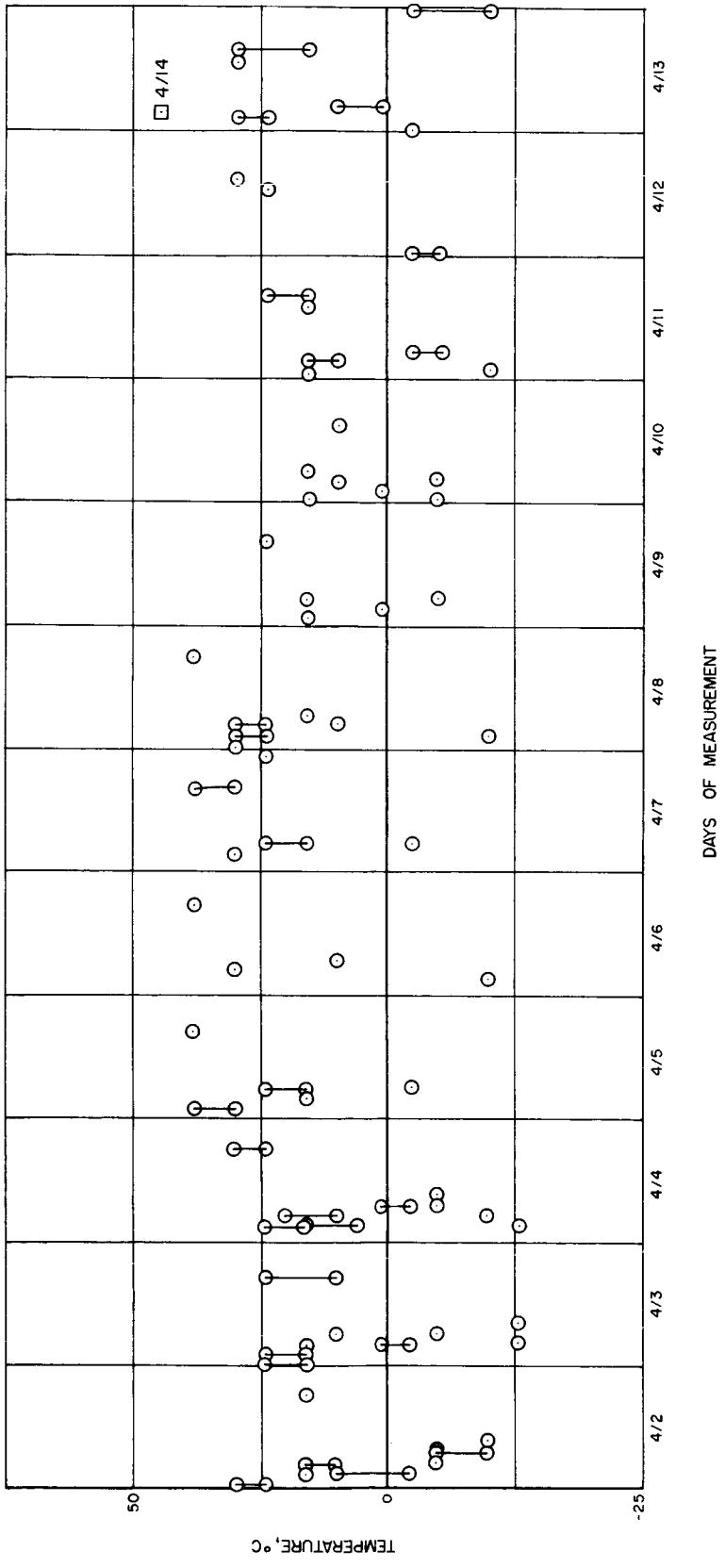

Fig. 17. Measured Cone Shell Temperature vs Time for 1958 ALPHA, April 2 through 13, 1958

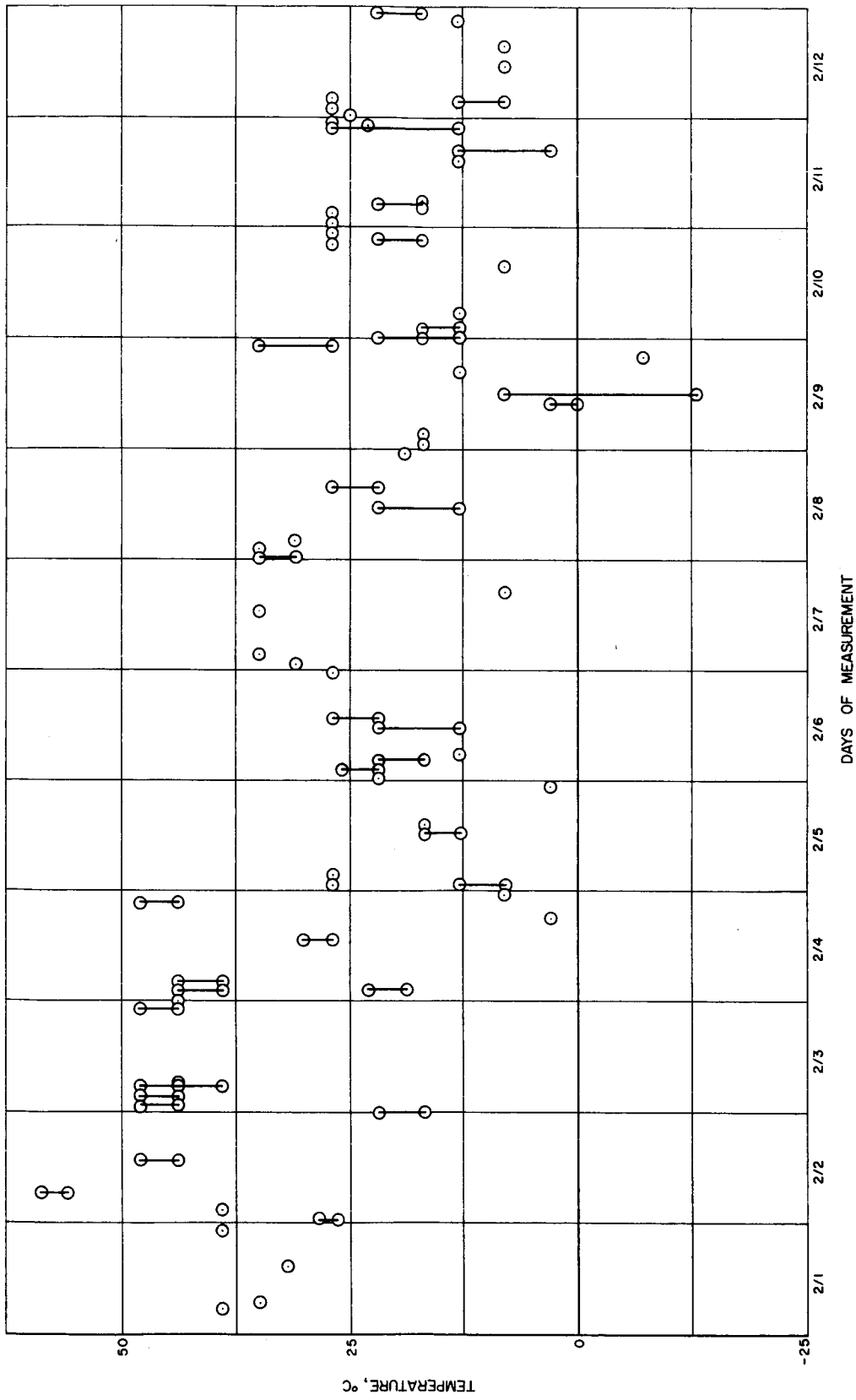

Fig. 18. Measured Stagnation Point Temperature vs Time for 1958 ALPHA, February 1 through 12, 1958

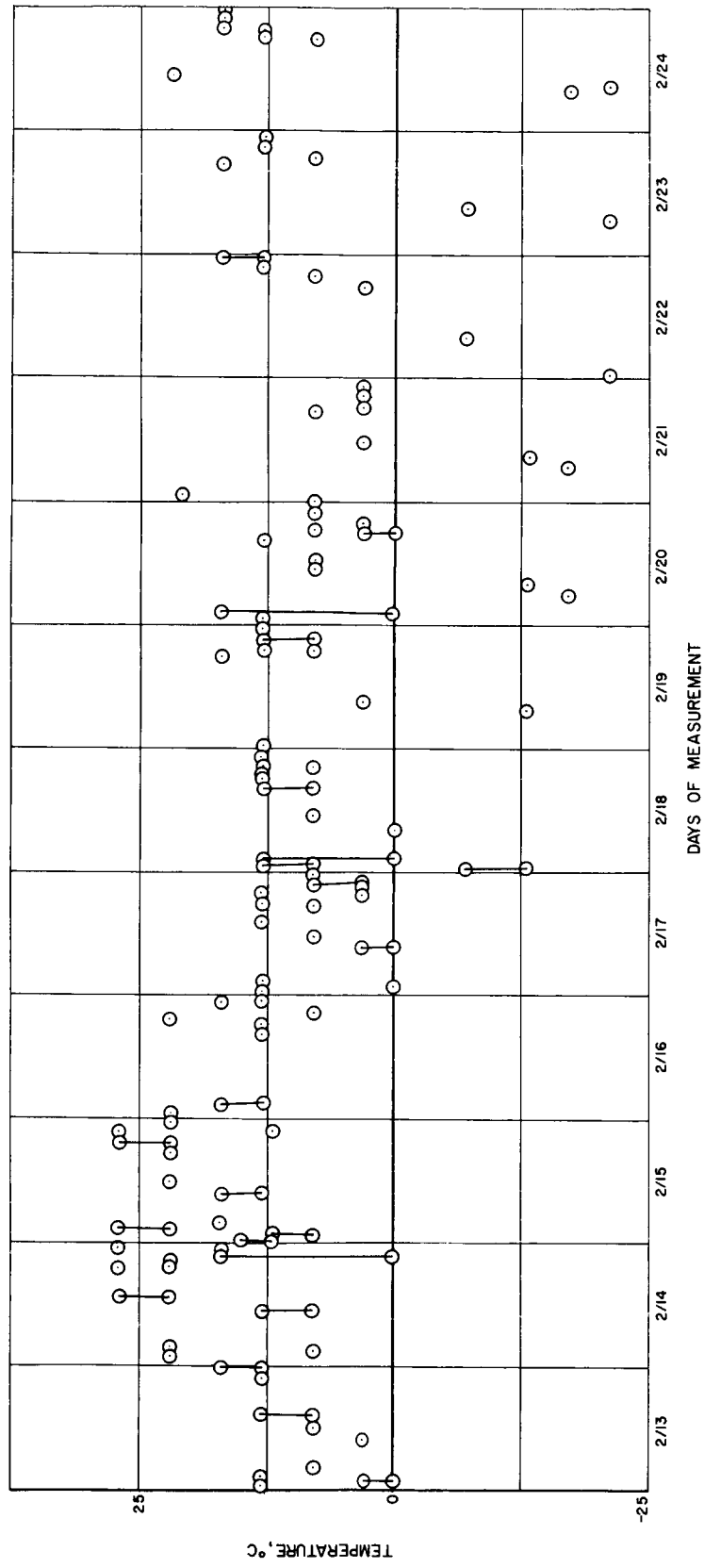

Fig. 19. Measured Stagnation Point Temperature vs Time for 1958 ALPHA, February 25 through March 8, 1958

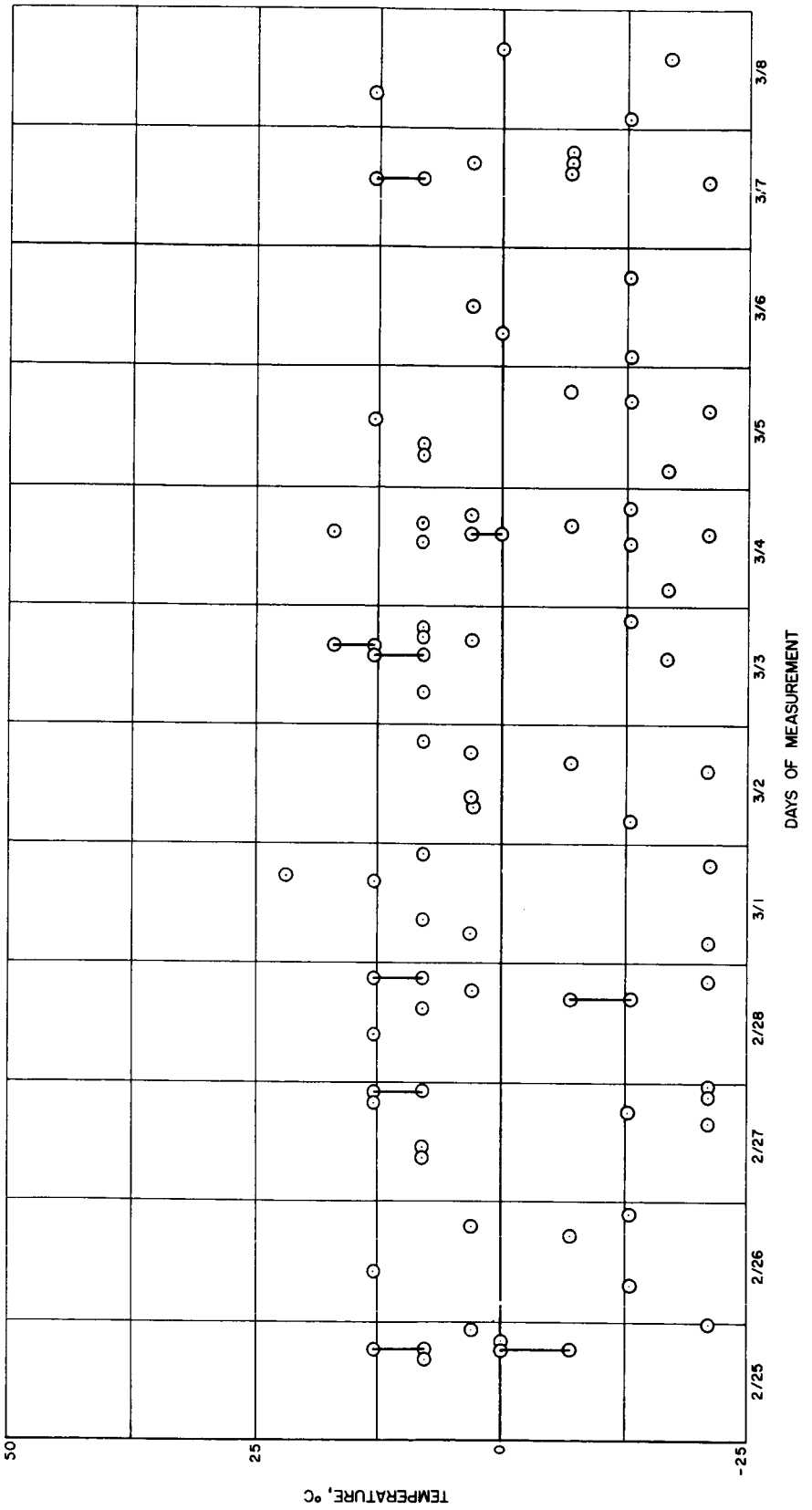

Fig. 20. Measured Stagnation Point Temperature vs Time for 1958 ALPHA, February 25 through March 8, 1958

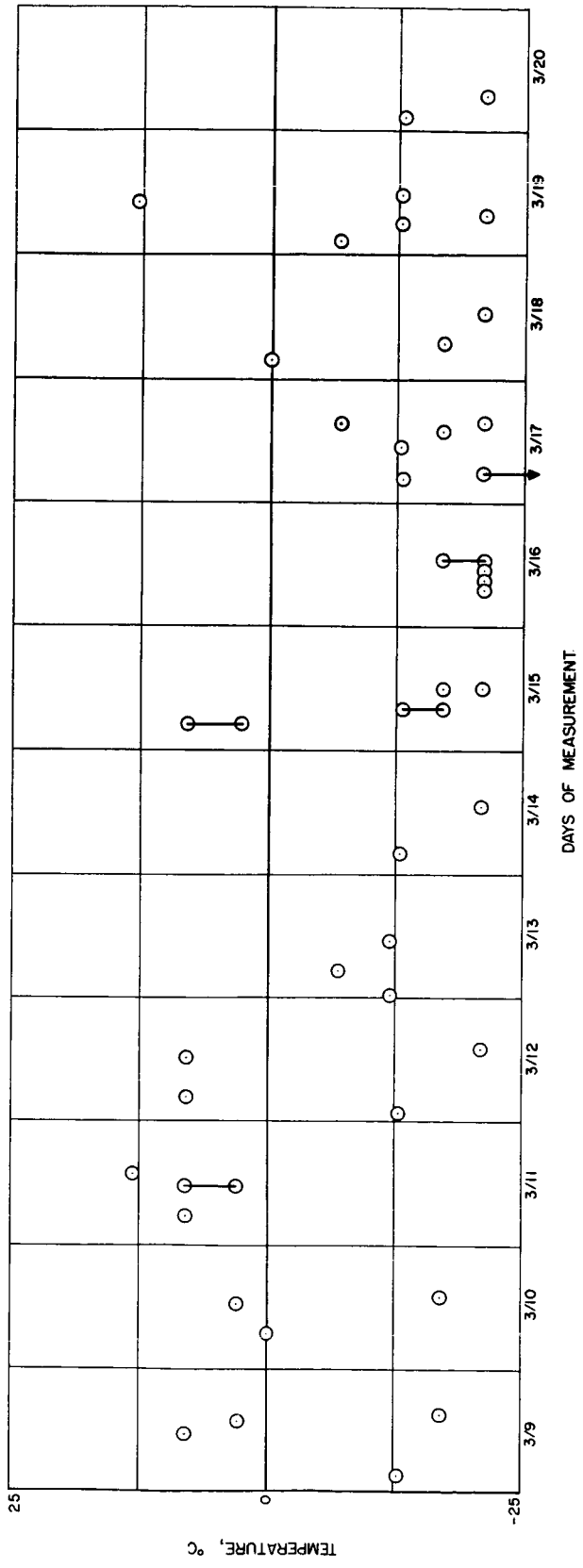

Fig. 21. Measured Stagnation Point Temperature vs Time for 1958 ALPHA, March 9 through 20, 1958

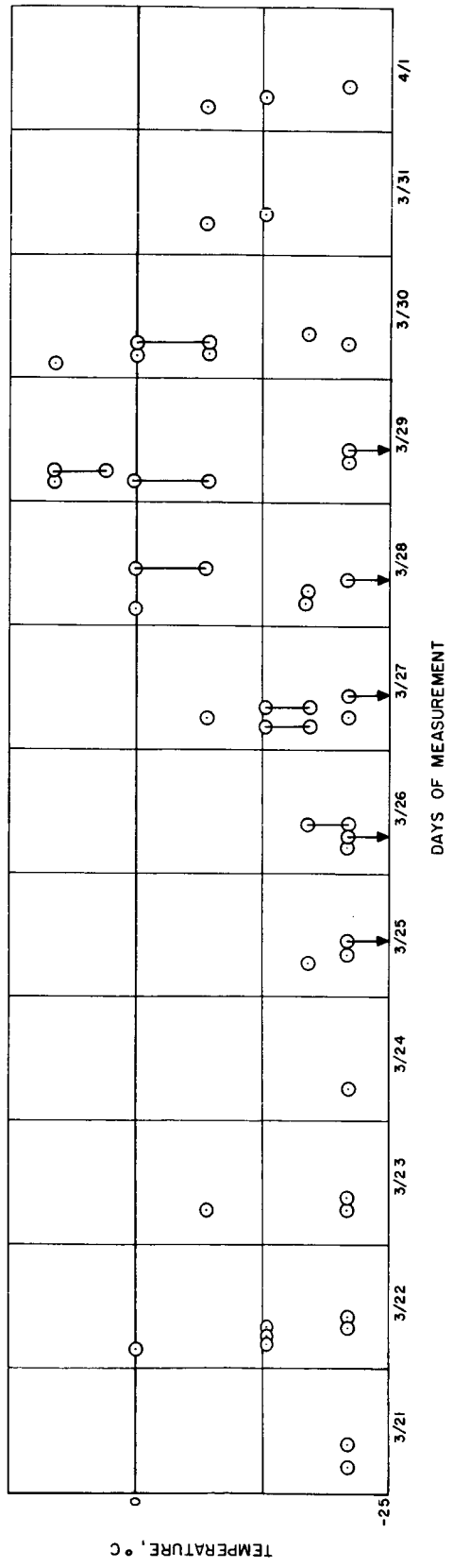

Fig. 22. Measured Stagnation Point Temperature vs Time for 1958 ALPHA, March 21 through April 1, 1958

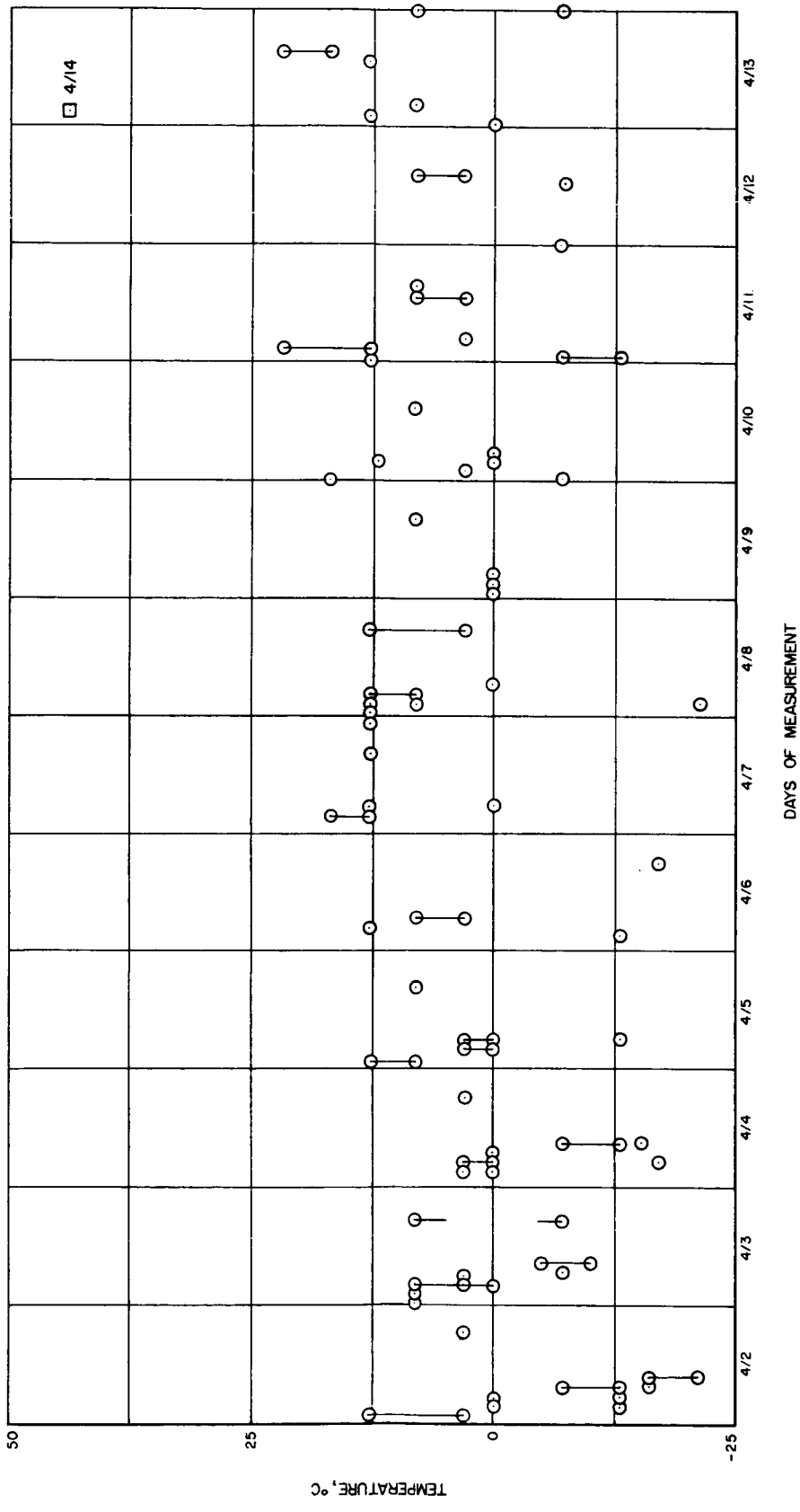

Fig. 23. Measured Stagnation Point Temperature vs Time for 1958 ALPHA
April 2 through 13, 1958

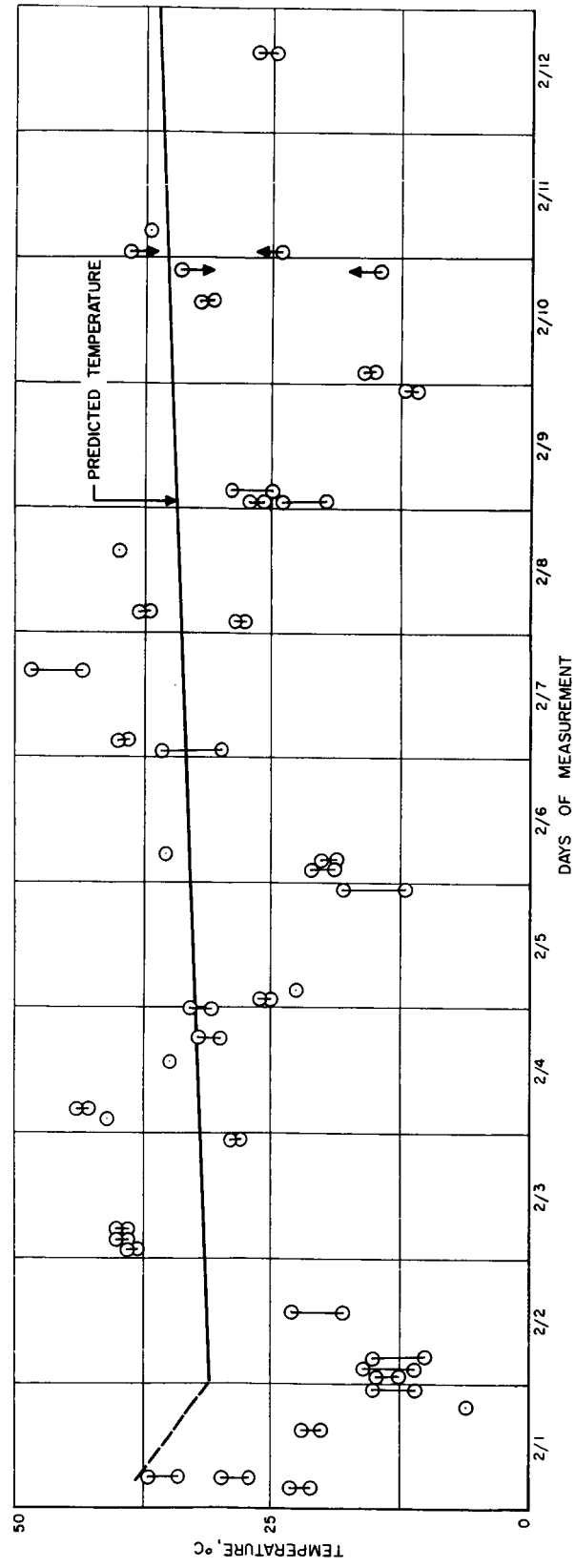

Fig. 24. Measured and Predicted Internal Cone Temperature vs Time for 1958 ALPHA, February 1 through 12, 1958

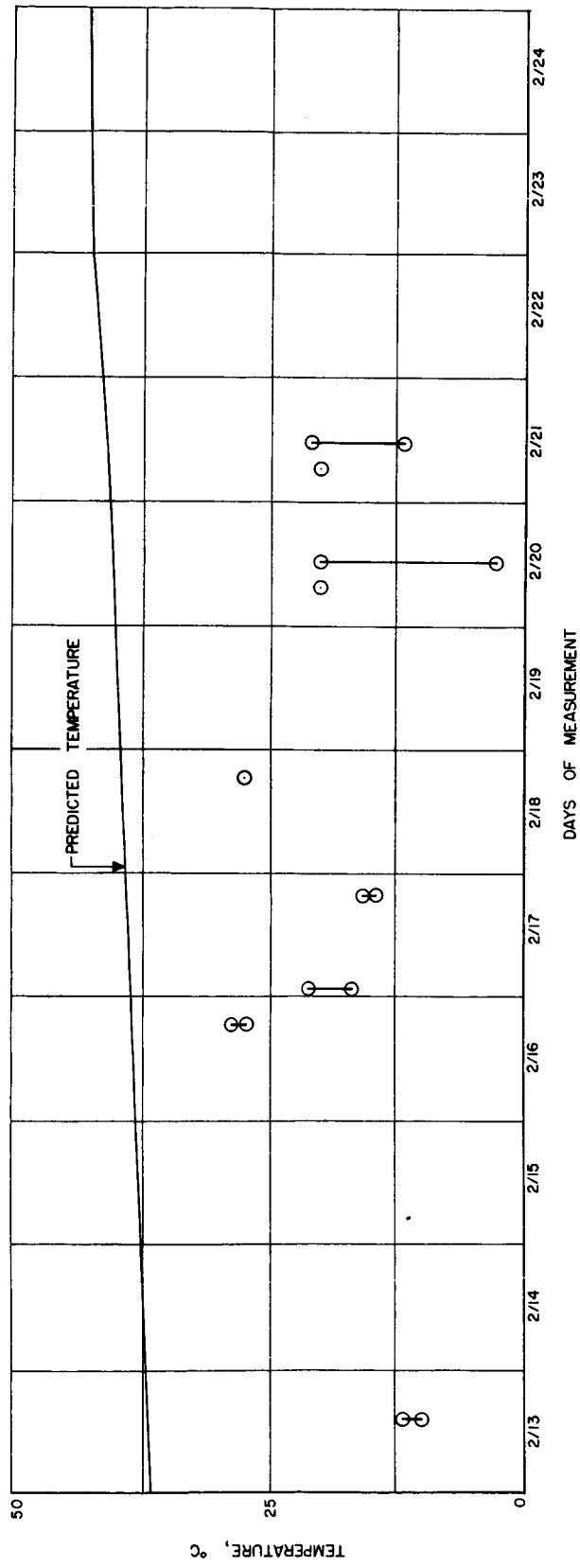

Fig. 25. Measured and Predicted Internal Cone Temperature vs Time for 1958 ALPHA, February 13 through 24, 1958

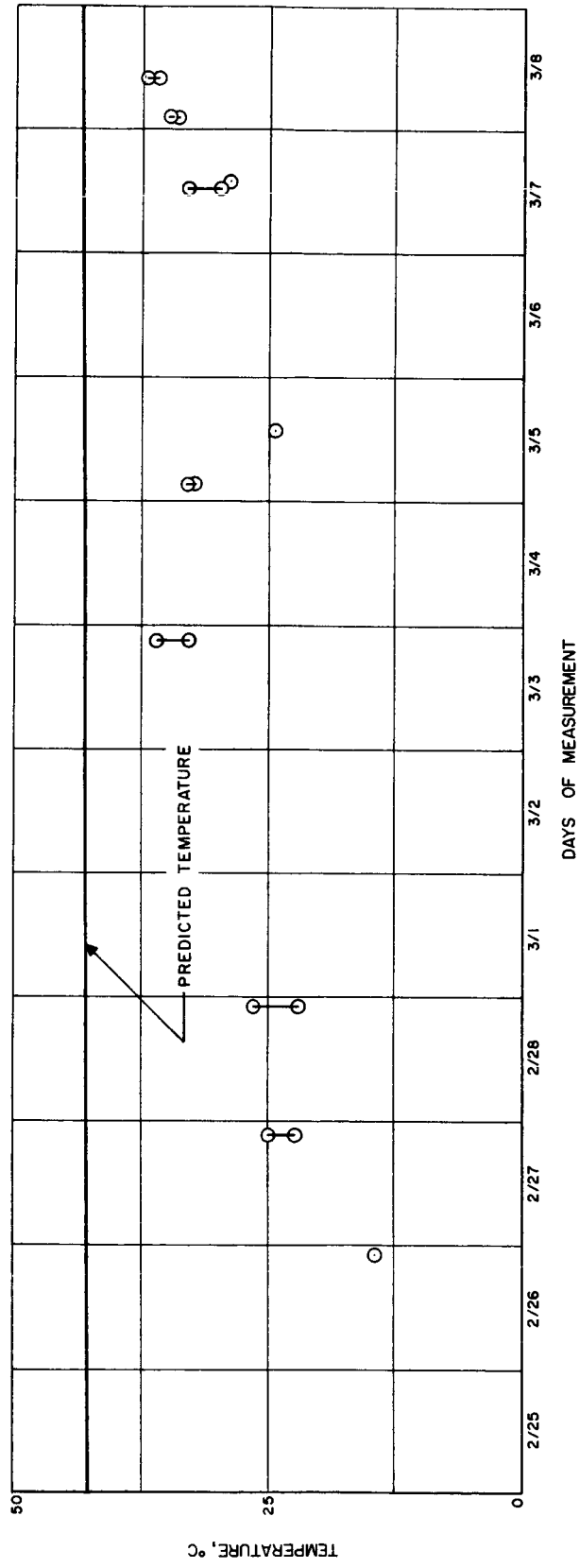

Fig. 26. Measured and Predicted Internal Cone Temperature vs Time for 1958 ALPHA, February 25 through March 8, 1958

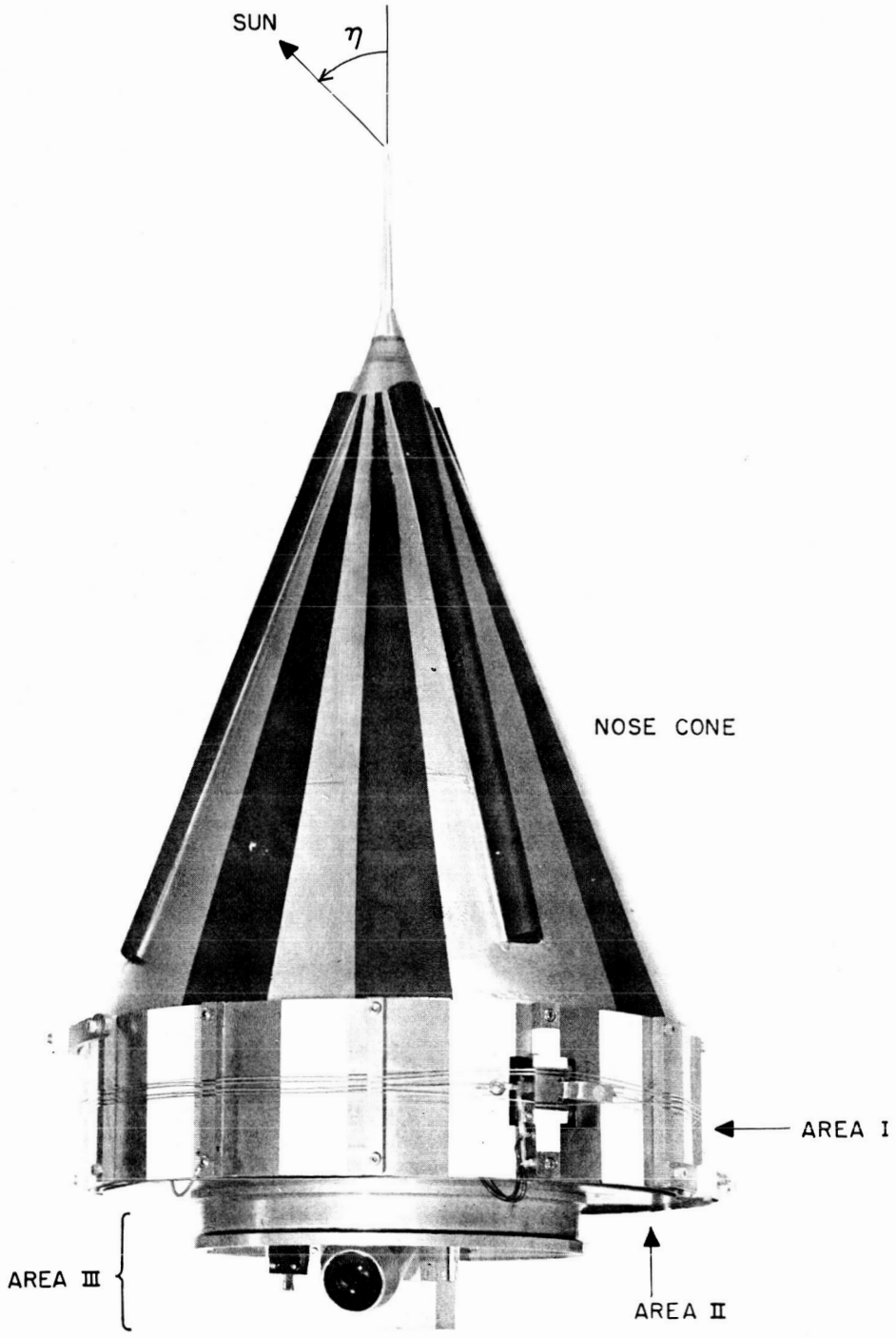

Fig. 27. Payload Configuration, PIONEERS III and IV

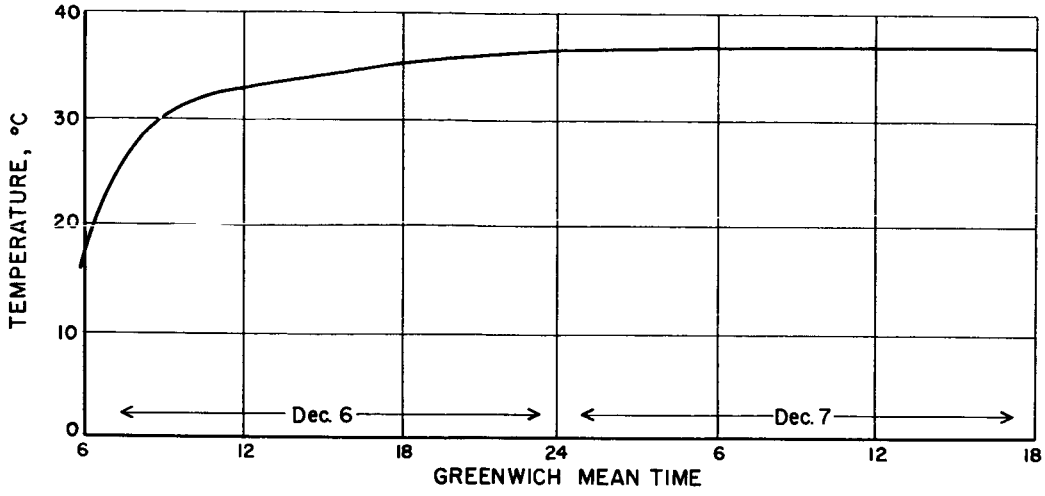

Fig. 28. PIONEER III Payload Temperature

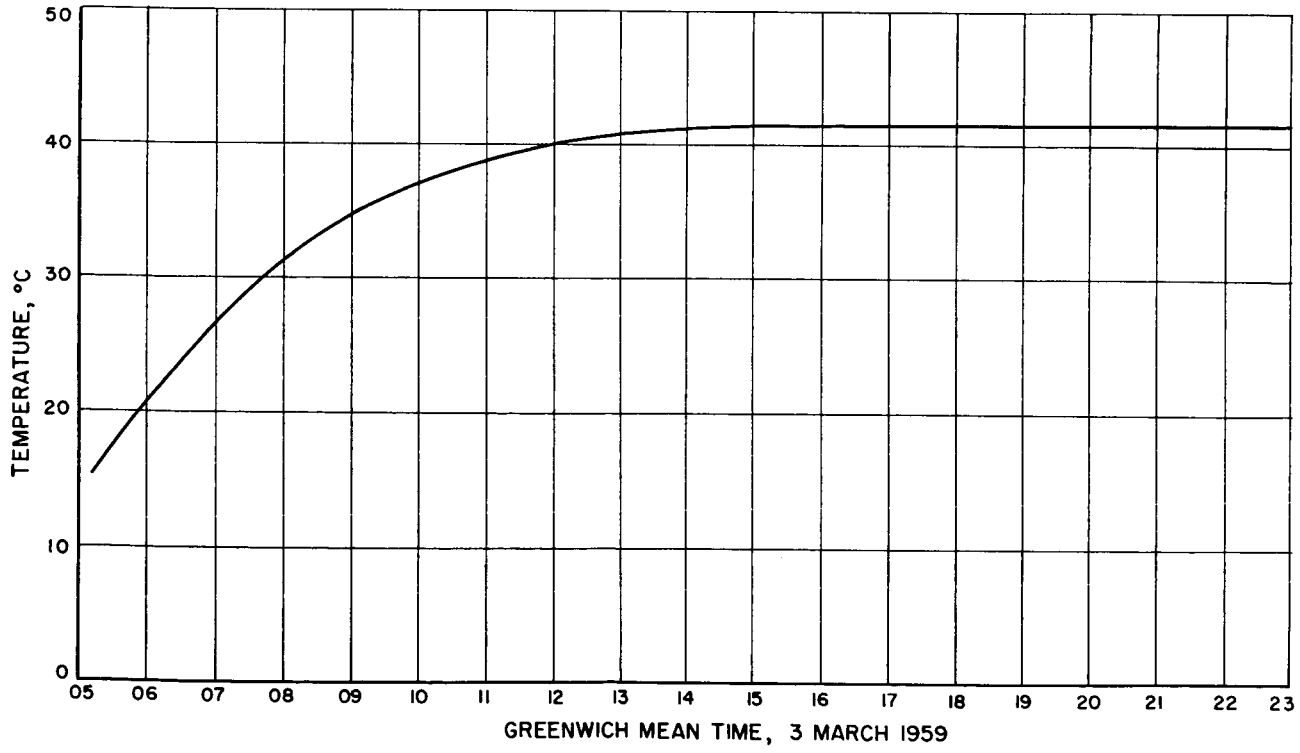

Fig. 29. PIONEER IV Payload Temperature

REFERENCES

1. Hibbs, A. R., The Temperature of an Orbiting Missile, Progress Report No. 20-294. Jet Propulsion Laboratory, Pasadena, California, March 28, 1956.

2. Goody, R. M., Physics of the Stratosphere, Cambridge University Press, New York, 1954.

3. Handbook of Chemistry and Physics, Chemical Rubber Publishing Company, Cleveland, Ohio, 1955.

4. Shipley, W. S., Evaluation of the Absorptivity of Surface Materials to Solar and Terrestrial Radiation, with Plots of the Reflectances (at Wavelengths of 0.4 to 25 μ), for Ten Sample Materials, Including Two Types of Fibrous-Glass-Reinforced Plastic, Progress Report No. 20-319. Jet Propulsion Laboratory, Pasadena, California, April 11, 1957.

5. Mechanical Engineers Handbook, McGraw-Hill Book Company, Incorporated, New York, 1941.

6. Randolph, L. W. and Choate, R. L., Calibration Record for the IGY Earth Satellite 1958 ALPHA, Publication No. 130. Jet Propulsion Laboratory, Pasadena, California, February 5, 1958.

7. Buwalda, E. P. and Hibbs, A. R., Satellite Temperature Measurements for 1958 ALPHA - EXPLORER I, ARS Paper 634-58. Presented at American Rocket Society Convention, Los Angeles, California, June 9, 1958.